CHAPTER IV NATURAL CONDITIONS IN AND AROUND THE PORT OF CALDERA

1. Topographical and Geological Features

1. 1 Topography

The Port of Caldera is situated at lat. 9°54'40"N. and long. 84°43'20"W. on the Pacific coast of the Republic of Costa Rica. The Port is a harbour constructed on the southeastern side of Caldera Bay which is situated on the east bank of the Gulf of Nicoya which opens to the south. The west side of the Port is largely sheltered by the Nicoya Peninsula 22 km away, and swells penetrating from the Pacific Ocean via the southern mouth of the Gulf of Nicoya are partially blocked by Cape Corralillo which projects out south of the Port of Caldera. Carballo Rock juts out north of the Port.

Directly behind the Port wharfs is a comparatively steep hilly district, the highest point of which is a more or less flat-topped mountain, Alto de las Mesas, which is approximately 140 m above sea-level.

Between the Port and Carballo Rock lies Caldera Beach a sandy beach area. Mata de Limón Estuary roughly bisects the bayside and is sheltered from the sea by a sand bar. The Jesús María River empties into the sea at the southern edge of Tivives, a beach which is situated to the south of Cape Coralillo. The Barranca River empties to the north of Carballo Rock. A sand bar, Puntarenas, approximately 7.5 km in length and 600 m in maximum width lies to the west of the Barranca River, and an urban area is developing westward over Puntarenas.

The location of the Port of Caldera and the topography of its surrounding area are shown in Fig. IV–1 and Fig. IV–2, respectively.

1. 2 Geology[1]

As shown in Table IV–1, the geography of the Port of Caldera area comprises the Tertiary Pre-Eocene bedrock of the Nicoya Group Formations, the Tertiary Miocene Cape Carballo Formations, and the Tivives and Orotina Formations which bridge the Pleiocene and Quaternary Pleistocene epochs. Quaternary Pleistocene diluvium and Holocene alluvium are distributed throughout the region, and cover all these geologic formations.

The Nicoya Group Formation consists of siliceous limestone and basalt. However, outcrops of these stones are not found in the Caldera Bay region. The Cape Carballo Formation consists principally of greyish blue sandstones and conglomerates, with bivalve fossils mixed in at places. Brown tuffaceous sandstones and mudstones alternations with basaltic pyroclastic layers are also found. These formations are widespread over the area and are locally exposed in the hilly area behind the wharf and in the hills in the vicinity of

---

1) Rodolfo Madrigal G : Geologia de Mapa Basico "Barranca", Casta Rica, Informes Tenicos y Notas Geologicas, Ciudad Universitaria "Rodorigo Facio", Casta Risa, 1970
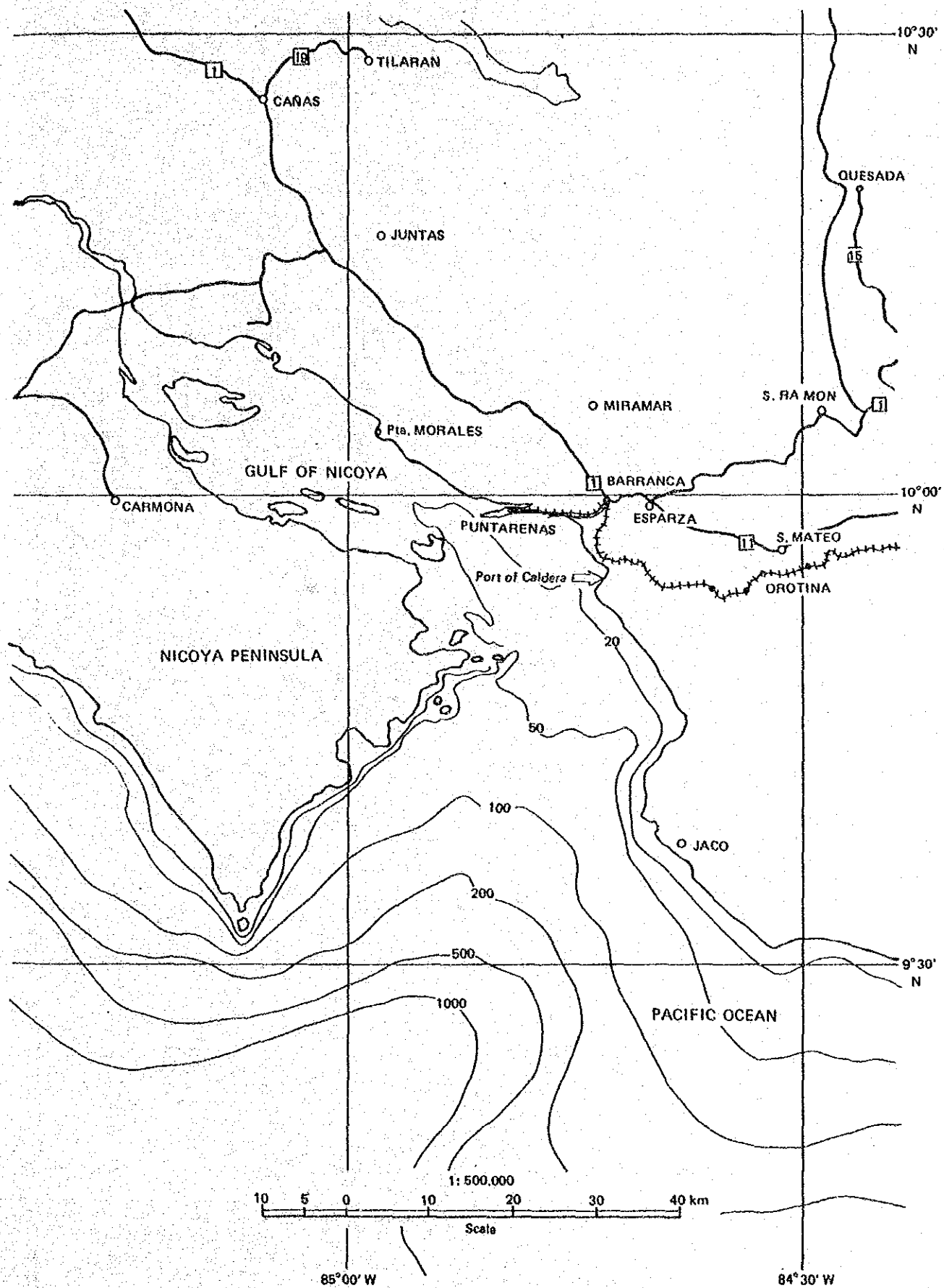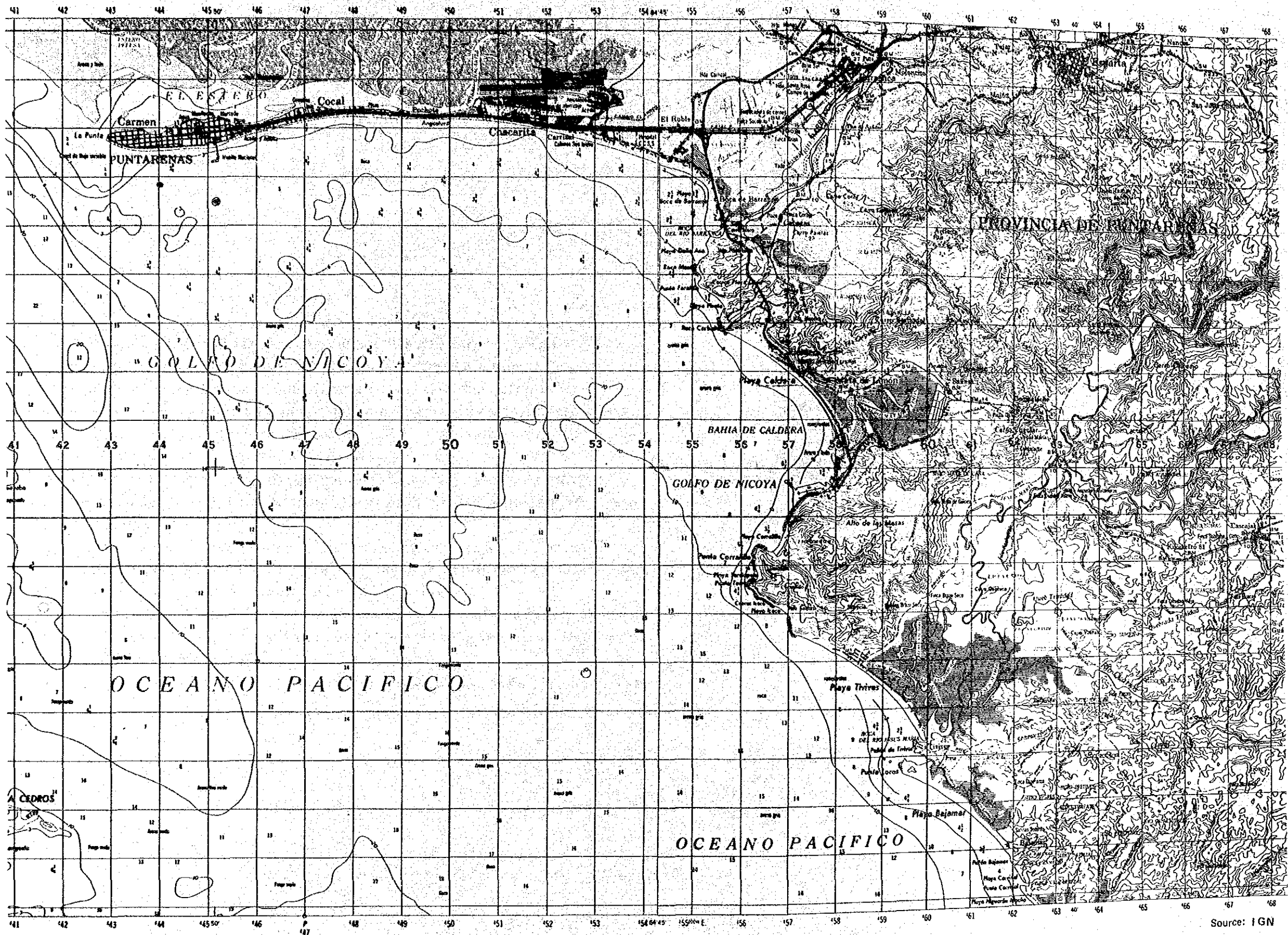
Fig. IV-1 Map of the Location of the Port of Caldera

Fig. IV-2 Topographical Map of the Port of Caldera and the Surrounding Region

Table IV-1 Geologic Formations is the Port of Caldera Region [1]

PERIOD	EPOCH	FORMATION
Quaternary	Holocene	Alluvium
	Pleistocene	Diluvium
		Orotina Formation
Tertiary	Pliocene	Tivives Formation
	Miocene	Cape Carballo Formation
	Pre-Eocene	Nicoya Group Formation

Source: Rodolfo Madrigal G.

Mata de Limón Station. The bedrock, described in Section 4 below is of a similar geologic formation. The Tivives Formation consists of agglomerates and lava flows. Depending on the spot, the massive agglomerates are interspersed with tuff and tuff-breccia. These formations are distributed at the peaks of the hills and behind the wharf. The Orotina Formation consists of welded tuff and is widespread in the hilly district on the left bank of the Jesús María River in the southwest.

The diluvium and alluvium consist of soft unconsolidated clay, sand, and gravel. They are found in the Mata de Limón Estuary flatlands, the river basins and plains, and the seabed of the Port of Caldera.

As stated above, the outermost stratum comprises a comparatively new Tertiary Period geologic formation which, in concert with the lack of river improvement, causes great efflusion of sand and becomes an abundant source of littoral drift.

Several faults running NE and NW are found in the area. The faults have been observed only in the Cape Carballo Formation regions, and are believed to have been created by the Central American Organic Movement.

The geologic formations of the Port of Caldera Region are shown in Fig. IV—3.
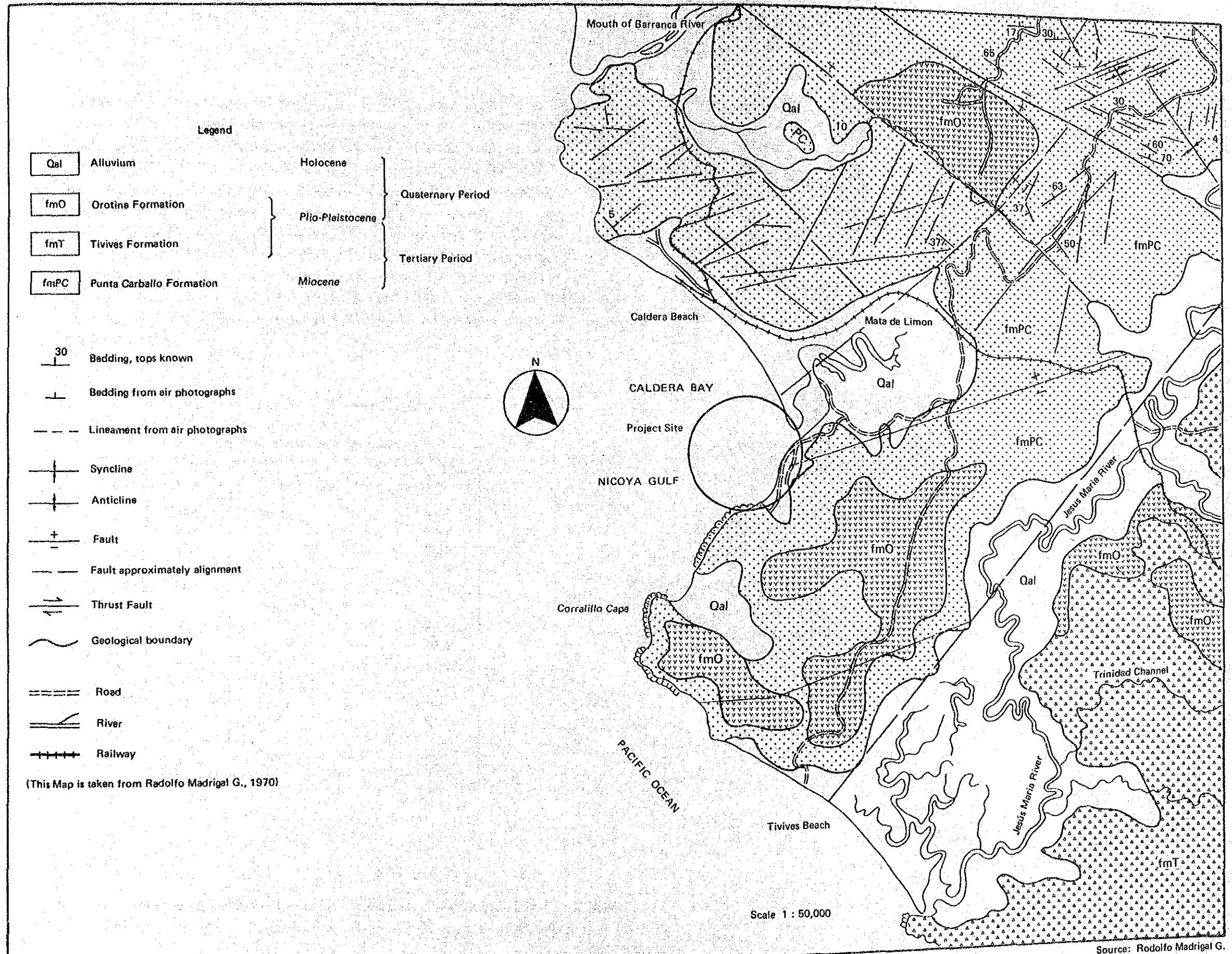
Legend

Qal	Alluvium
fmO	Orotina Formation
fmT	Tivives Formation
fmPC	Punta Carballo Formation

Holocene

Pilo-Pleistocene

Miocene

Quaternary Period

Tertiary Period

30 ⊥ Bedding, tops known

⊥ Bedding from air photographs

— — — Lineament from air photographs

Syncline

Anticline

Fault

Fault approximately alignment

Thrust Fault

Geological boundary

Road

River

Railway

(This Map is taken from Radolfo Madrigal G., 1970)

Mouth of Barranca River

Caldera Beach

Mata de Limon

CALDERA BAY

Project Site

NICOYA GULF

Corralillo Cape

PACIFIC OCEAN

Tivives Beach

Trinidad Channel

Jesus Maria River

Jesús Maria River

Scale 1 : 50,000

Source: Rodolfo Madrigal G.

Fig. IV-3 Geological Map of the Port of Caldera and the Surrounding Region

2. Meteorological Conditions

2.1 Temperature

The distribution of mean annual temperature in Costa Rica based on a twenty year record from 1961 to 1980 is shown in Fig. IV—4. As may be seen in the figure, the mean temperatures in the Pacific and Caribbean coast regions are higher than the mean temperature of 17.5°C to 20°C recorded in the central highlands which include the Capital, San José. A particularly high mean temperature of approximately 27.5°C was recorded on the east shore region of the Gulf of Nicoya which includes the Port of Caldera.

Table IV—2 shows the mean values by month of the maximum, minimum, and mean temperatures in Puntarenas over a 20 year period from 1965 to 1984. Puntarenas is situated approximately 15 km west-northwest of the Port of Caldera. The table shows high temperatures in March and April, and low temperatures from September to December. However, the temperature variation throughout the year is small with the mean temperature ranging between 26°C and 29°C.

Table IV-2 Monthly Mean Values of Maximum,
Minimum and Mean
Temperatures in Puntarenas
(Average Over Twenty Years from 1965 to 1984 ; Unit : °C)

Month	Max. Temp.	Min. Temp.	Mean Temp.
Jan.	33.6	21.6	27.1
Feb.	34.5	21.9	27.7
Mar.	35.3	22.6	28.1
Apr.	34.9	23.5	28.5
May	33.2	23.6	27.6
Jun.	32.4	23.3	26.9
Jul.	32.5	22.9	26.8
Aug.	32.6	22.8	26.6
Sep.	32.1	22.8	26.4
Oct.	31.5	22.8	26.2
Nov.	31.8	22.4	26.3
Dec.	32.5	21.5	26.5
Annual Mean	33.1	22.6	27.1

Source : IMN

2.2 Precipitation

The distribution of mean annual precipitation in Costa Rica is shown in Fig. IV—5 based on the record from 1961 to 1980. Precipitation along the Nicoya Gulf Coast region is
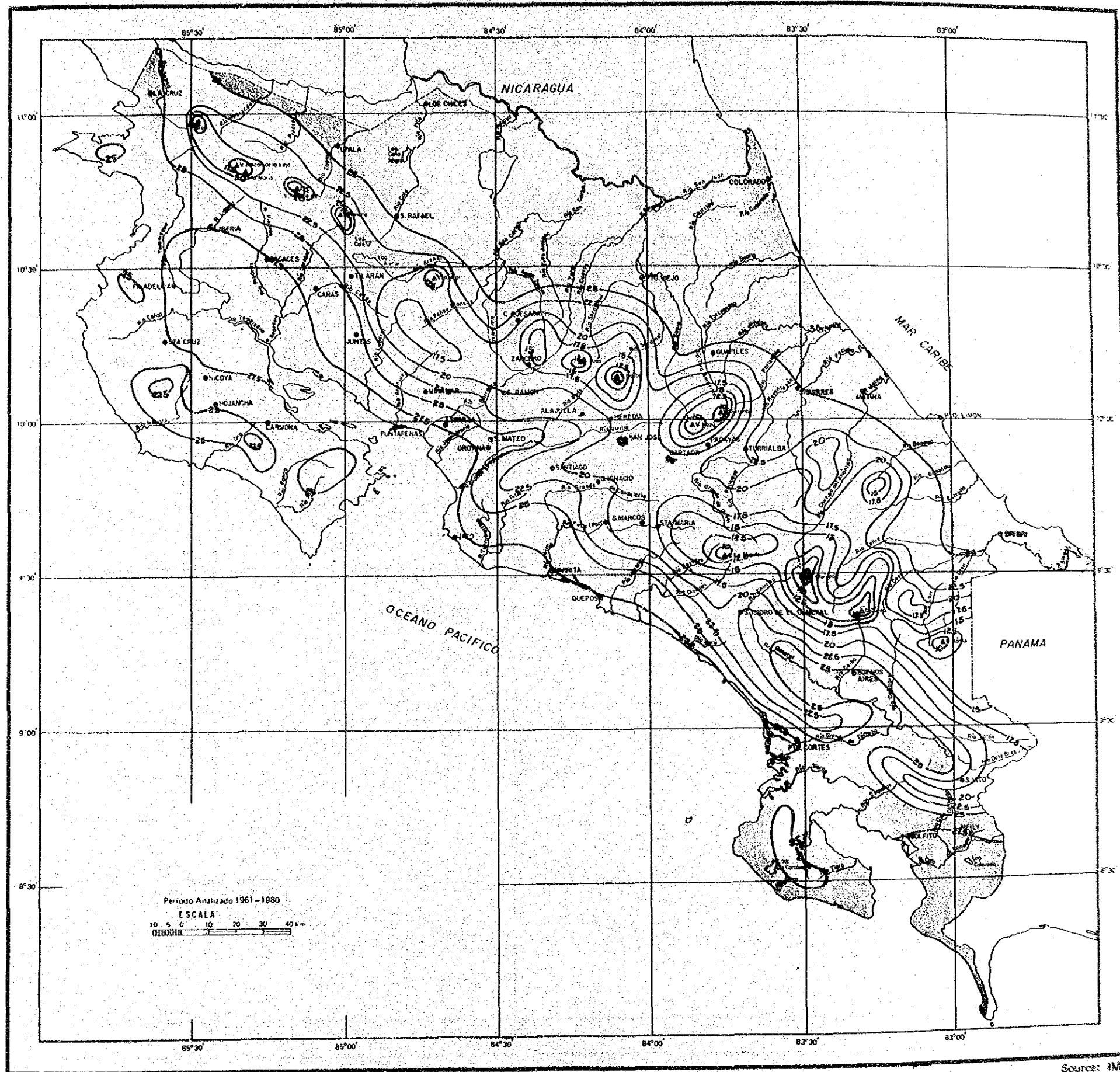
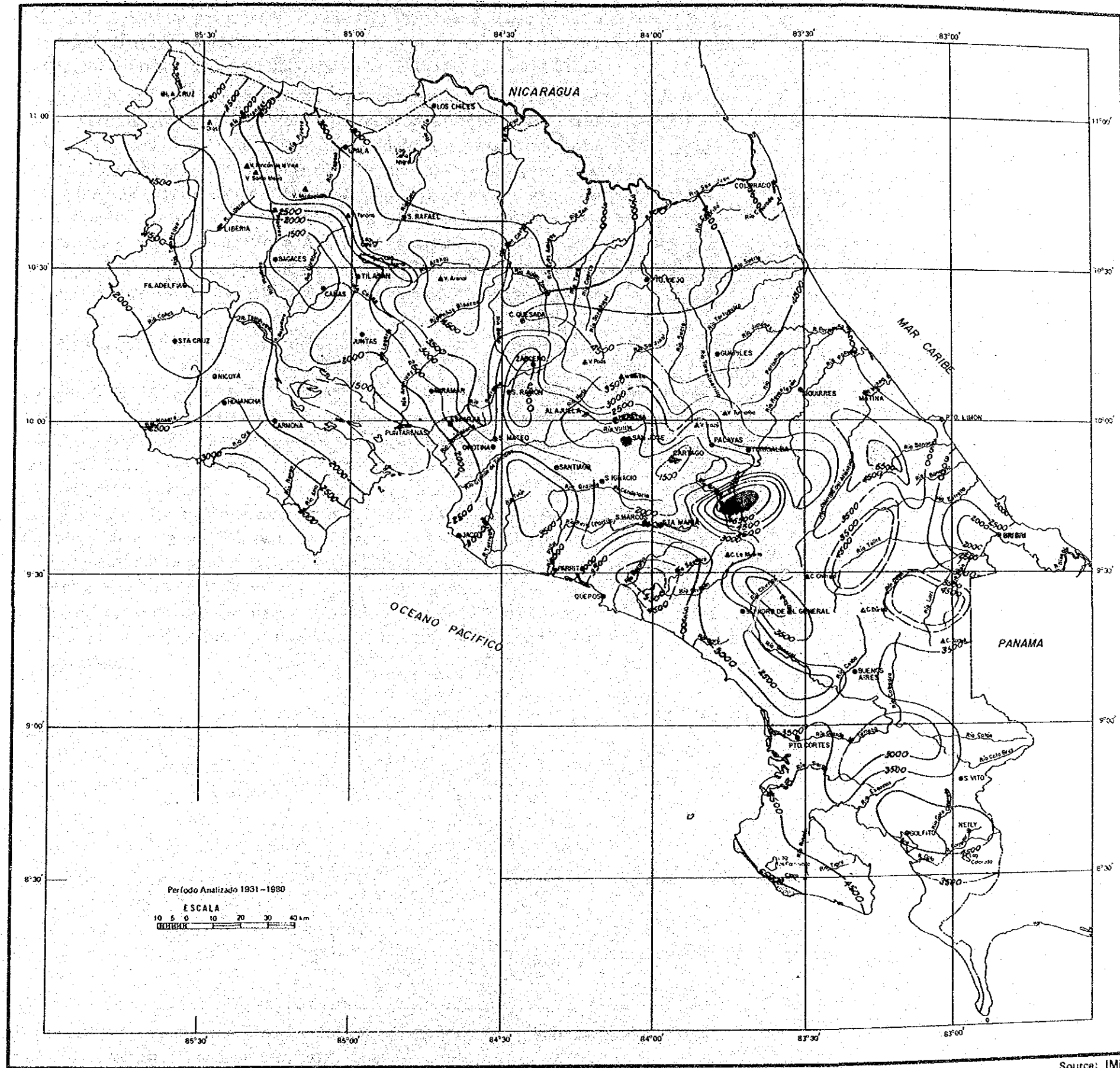**Fig. IV-4 Annual Mean Temperature Distribution in Costa Rica**

Fig. IV-5 Annual Mean Precipitation Distribution in Costa Rica

approximately 1,600 mm per annum. Along with the central plateau this region has the lowest precipitation in Costa Rica.

The monthly precipitation in Puntarenas over a twenty year period from 1964 to 1984 is shown in Table IV-3 (In 1968, the six months from May to October were improperly measured, hence the year 1968 is omitted from the record.). The mean annual precipitation during this period was 1,677 mm. A maximum single year precipitation of 2,115 mm was recorded in 1981 and a minimum value of 1,081 mm was recorded in 1965. As may be verified by the table, there is a clear demarcation between the rainy season (winter) which lasts from May to November and the dry season (summer) which lasts from December to April. The rainy season months from August to October see particularly heavy rainfall. During this period, rainfall from afternoon to evening is normal. On the other hand, there is virtually no precipitation during the dry season months from January to March.

2. 3 Wind

Fig. IV-6 shows hourly wind direction and wind speed percentages by month at Chacarita Airport in Puntarenas based on wind measurement records from 1970 to 1971[2]. Fig. IV-7 shows the distribution of mean wind speeds (unit : km/h) in prevailing wind directions and in all wind directions, plotted by month and hour.

According to the figures, northerly, northeasterly and easterly land breezes and trade-winds prevail during the nighttime hours from 7 PM to 8 AM. During the day, southerly and southwesterly winds prevail. These are sea breezes and equatorial westwinds. The winds in the dry season from December to April are sea breezes. However, during the rainy season when equatorial west winds blow, sea breezes and equatorial west winds intermingle. Between June and February, southeasterly winds prevail between 5 PM and 8 PM.

Wind speed is high during the day, and particularly so during the dry season from December to May.

2) Eladio Zarate H.; Comportamiento del Viento en Costa Rica, Nota de Investigación, No. 2, Instituto Meteorológico Nacional, Dec. 1978, 31 p.

Table IV-3 Monthly Precipitation in Puntarenas
(1964 – 1984; Unit : mm)

| Year	Jan.	Feb.	Mar.	Apr.	May	Jun.	Jul.	Aug.	Sep.	Oct.	Nov.	Dec.	Total
1964	0.0	0.0	0.0	81.0	93.9	320.2	251.6	209.6	—	—	59.2	56.5	1072.0
1965	0.0	0.0	0.0	0.0	105.0	166.7	158.8	198.8	286.1	73.7	72.5	19.5	1080.8
1966	0.0	0.0	34.5	0.0	343.0	312.5	122.4	219.0	122.3	417.2	42.1	17.9	1630.9
1967	0.3	14.5	0.0	88.9	39.0	248.2	266.5	90.6	372.1	191.8	29.6	98.3	1440.4
1969	2.5	0.0	1.2	12.0	134.8	253.1	124.6	364.6	319.0	357.7	250.5	0.3	1820.3
1970	13.0	2.9	29.8	43.8	167.6	147.6	417.3	321.2	269.5	418.8	38.5	61.0	1931.0
1971	0.3	1.3	13.6	95.9	448.7	203.5	53.3	317.6	455.1	178.5	83.4	1.8	1853.1
1972	35.3	0.0	0.9	29.6	289.6	140.6	81.8	384.9	469.2	330.4	208.5	108.8	2079.6
1973	0.0	—	1.5	18.6	307.6	266.7	166.4	496.0	403.3	290.3	77.1	0.0	2027.5
1974	0.0	0.0	11.4	39.7	133.2	197.8	136.3	262.8	587.1	213.1	9.3	9.5	1600.2
1975	0.0	1.4	16.5	0.0	108.3	168.8	224.9	334.3	374.3	163.3	239.7	17.0	1648.5
1976	0.0	0.0	0.0	2.6	157.6	376.4	33.6	142.3	140.3	237.7	176.3	0.8	1268.2
1977	0.0	0.0	0.0	15.5	61.6	261.8	117.2	181.9	313.0	199.6	181.8	10.9	1343.3
1978	0.0	0.0	0.0	10.3	220.4	141.7	206.7	255.1	196.0	309.1	49.3	50.0	1129.5
1979	0.0	0.0	0.0	41.3	158.8	321.7	116.5	622.3	341.5	366.9	84.1	14.8	2067.9
1980	58.4	9.7	0.0	21.9	193.7	160.4	172.0	123.1	233.8	395.5	248.4	36.4	1654.3
1981	0.0	0.0	5.3	96.8	508.4	503.4	151.2	325.5	249.8	225.9	63.6	87.2	2215.1
1982	51.0	0.0	0.0	18.8	502.3	166.6	155.7	46.1	315.3	152.0	76.3	0.0	1484.1
1983	0.0	4.7	15.3	35.9	48.4	348.6	303.9	278.1	347.6	265.9	152.6	148.0	1949.0
1984	0.0	23.0	6.9	62.6	345.0	159.8	200.1	182.2	254.2	82.8	42.5	0.4	1359.5
Mean	8.1	3.0	6.8	35.3	218.2	243.3	173.0	267.8	318.4	256.3	109.3	37.0	1677.0

Source:IMN
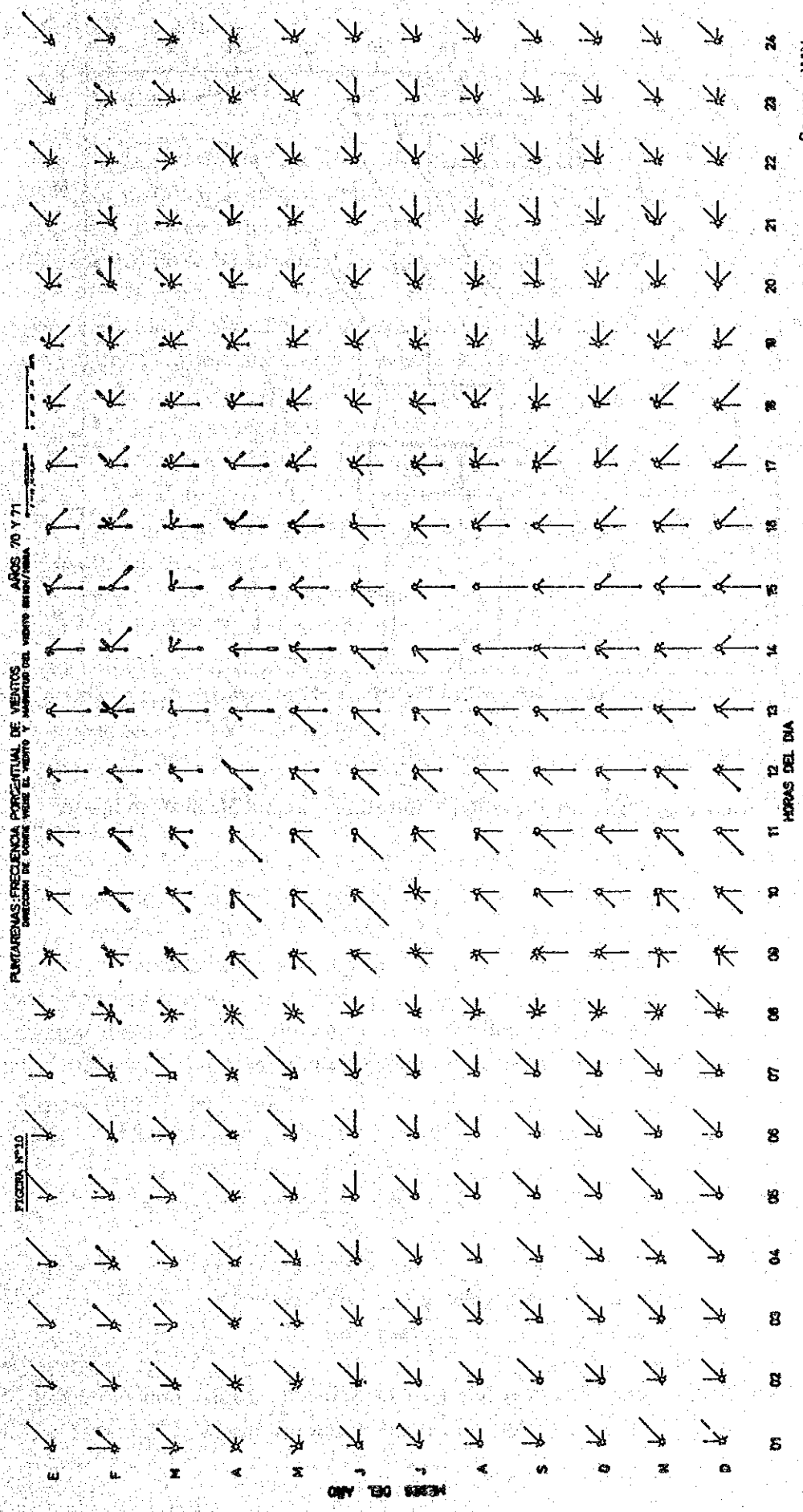
Fig. IV-6 Hourly and Monthly Wind Direction and Wind Speed Distribution at Puntarenas
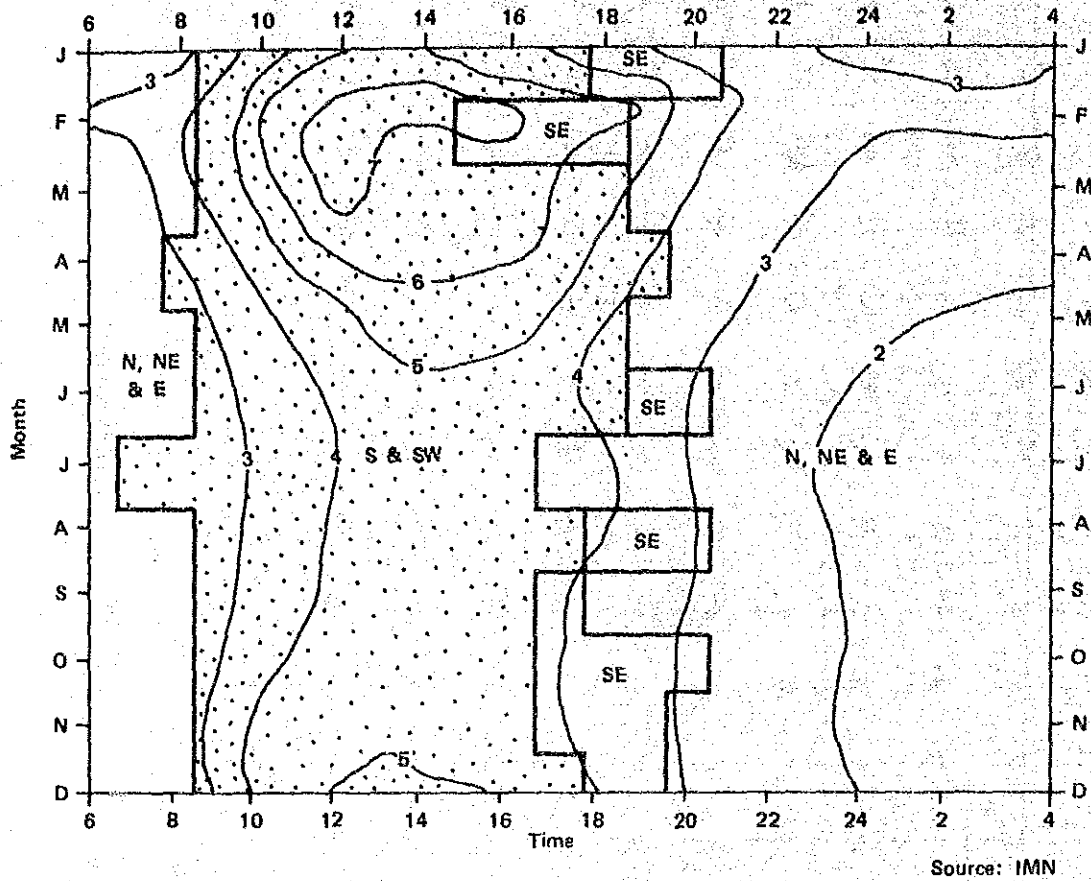
Source: IMN

—93—

Fig. IV-7   Hourly and Monthly Prevailing Wind Direction and Mean Wind Speed

3. Marine Conditions

3. 1　Wave Conditions

　　Wave observation at the Port of Caldera began on June 15, 1978 using an ultrasonic wavemeter installed at a spot approximately 1.8 km offshore at a waterdepth of −13.5 m. This observation continues to the present. (Refer to Fig. IV−8). The periods in which data were obtained up to November 14, 1985 are shown in Fig. IV−9. During a wave observation period of 7.3 years, there were 3.3 years for which data were obtained. In July 1980, a significant wave calculation apparatus was furnished and significant wave height, maximum wave height, 1/10 maximum wave height, and mean wave height, as well as their respective periods, were automatically calculated and displayed.

　　Table IV−4 was prepared based on the record during the observation period, and shows the crossing frequency table between significant wave height and significant wave period. Fig. IV−10 and Fig. IV−11 show cumulative probable distribution of significant wave height and significant wave period respectively. The probability of significant wave heights between 0.5 m and 1.0 m is 65.4%. Ninety percent of significant wave heights are between 0.5 m and 1.5 m. 87.3% of significant wave periods are 9.5 s or greater. Dr. Goda, Director General of the PHRI, infers that this type of long period swell is generated in the long distance wind regions formed along the pressure incline between extensive high pressure and low pressure formations which are found in the South Pacific region between lat. 50° to 60°S. and long. 120° to 160°W. Accordingly, it is estimated that these waves are propagated over distances of 7,000 km to 9,000 km[3]. It is believed, therefore, that the directional dispersion of the waves is extremely small and that the waves exhibit behavior approaching that of regular waves.

　　Table IV−5 is a ranking in descending order of extremely large waves of a significant wave height greater than 1.5 m recorded during the observation period. Using the data of the 29 waves of significant wave height greater than 1.8 m, suitable probable wave heights and their corresponding periods which are estimated using the 3.3 year period in which data were obtained are shown in Table IV−6. The probable wave heights were calculated by adapting the above data to Gumbel and Weibull distributions, selecting the functions most compatible with the data, and extrapolating an equation for the inferred relationship. The distribution with the highest level of compatibility is a Weibull distribution with an exponent of 1.25, the equation for which is stated below.

$$P[H \leqq x] = 1 - \exp\left[-\left(\frac{x - 1.694}{0.689} \right)^{1.25} \right]$$

Where,　　　H : wave height (m)

　　　　　　x : wave height of a certain fixed value (m)

　　　　$P[H \leqq x]$: probability that wave height H will not exceed x

---

3) Yoshimi Goda; Analysis of Wave Grouping and Spectra of Long-travelled Swell, Report of the Port and Harbour Research Institute, Vol. 22, No. 1, March 1983, pp. 3 ～ 41.
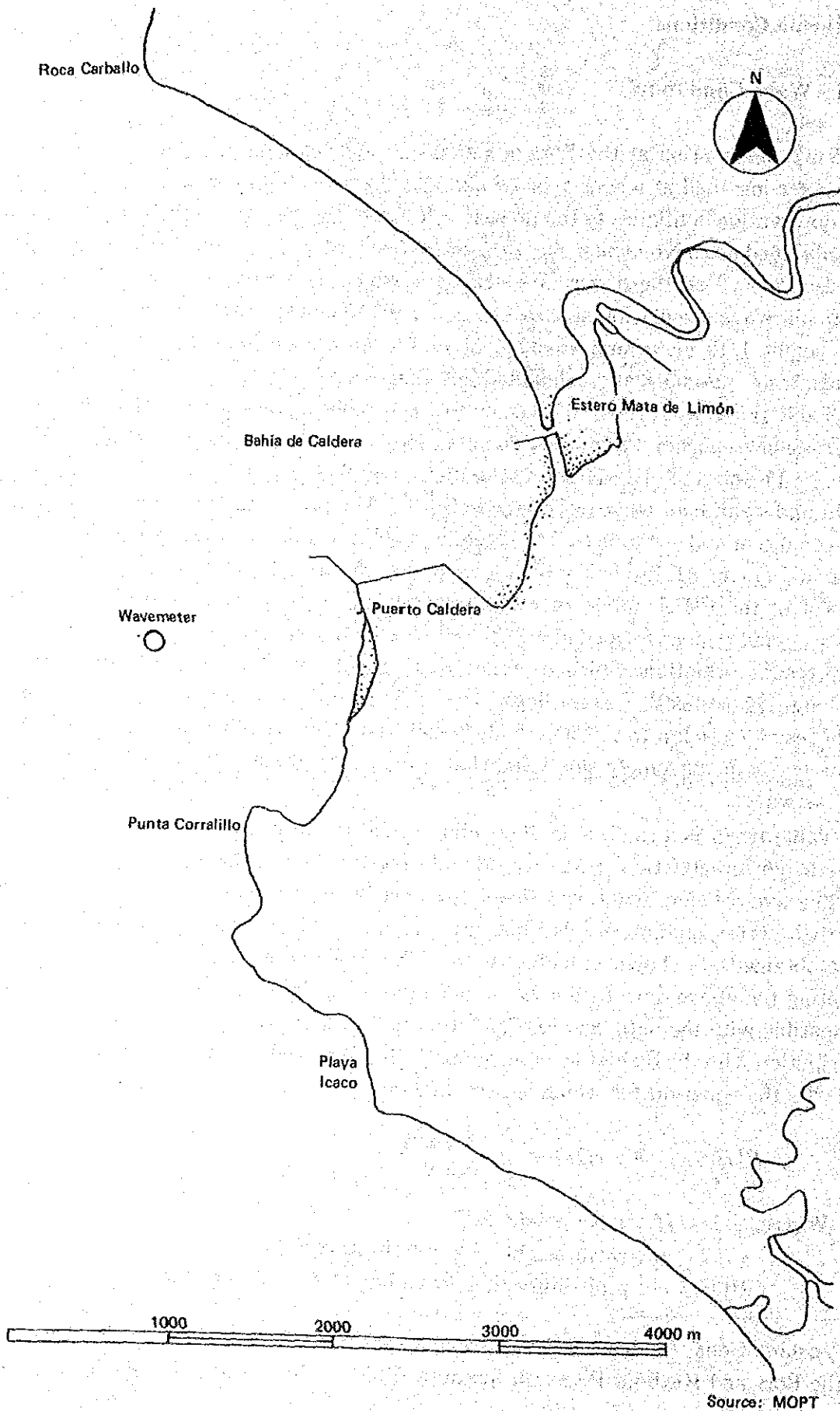
Roca Carballo

N

Estero Mata de Limón

Bahía de Caldera

Wavemeter
O

Puerto Caldera

Punta Corralillo

Playa
Icaco

1000   2000   3000   4000 m

Source: MOPT

Fig. IV-8 Location Map of Wavemeter

Fig. IV-9 Period of Wave Observation

Source: MOPT

Table IV-4 Wave Occurance Probability by Significant Wave Height and Significant Wave Period

(Observation Period : June 15, 1978~Nov. 14, 1985 ; Ratio of Observed Waves : 45.2%)

| $H_{1/3}$ (m)	$T_{1/3}$ (s)	≦3.5	3.5~4.5	4.5~5.5	5.5~6.5	6.5~7.5	7.5~8.5	8.5~9.5	9.5~10.5	10.5~11.5	11.5~12.5	12.5~13.5	13.5~14.5	14.5~15.5	15.5~16.5	16.5~17.5	17.5~18.5	18.5<	Total	Cumulative Probability (%)
≦0.5	Frequency				8	26	46	66	112	141	104	80	41	15	19	6	3	2	669	5.8
	Probability				0.1	0.2	0.4	0.6	1.0	1.2	0.9	0.7	0.4	0.1	0.2	0.1	0.0	0.0	5.8	
0.5~1.0	Frequency	2	3	11	38	132	357	689	1020	1340	1390	1211	821	346	98	28	12	8	7506	71.3
	Probability	0.0	0.0	0.1	0.3	1.2	3.1	6.0	8.9	11.7	12.1	10.6	7.2	3.0	0.9	0.2	0.1	0.1	65.4	
1.0~1.5	Frequency	1	1	1	5	14	15	39	119	191	352	544	634	435	187	74	15	5	2631	94.2
	Probability	0.0	0.0	0.0	0.0	0.1	0.1	0.3	1.0	1.7	3.1	4.7	5.5	3.8	1.6	0.6	0.1	0.0	22.9	
1.5~2.0	Frequency	1						3	5	9	15	34	82	145	93	44	18	6	455	98.2
	Probability	0.0						0.0	0.0	0.1	0.1	0.3	0.4	1.3	0.8	0.4	0.2	0.1	4.0	
2.0~2.5	Frequency						1	2	1				4	24	49	35	14	5	135	99.3
	Probability						0.0	0.0	0.0				0.0	0.2	0.4	0.3	0.1	0.0	1.2	
2.5~3.0	Frequency													1	10	27	9	4	51	99.8
	Probability													0.0	0.1	0.2	0.1	0.0	0.4	
3.0~3.5	Frequency														2	14	8		24	100.0
	Probability														0.0	0.1	0.1		0.2	
3.5~4.0	Frequency															1			1	100.0
	Probability															0.0			0.0	
4.0<	Frequency																			
	Probability																			
Total	Frequency	3	4	12	51	172	419	799	1257	1681	1861	1869	1582	966	458	228	80	30	11,472	
	Probability	0.0	0.0	0.1	0.4	1.5	3.7	7.0	11.0	14.7	16.2	16.3	13.8	8.4	4.0	2.0	0.7	0.3	100.0	
Cumulative % Probability		0.0	0.1	0.2	0.6	2.1	5.8	12.7	23.7	38.4	54.6	70.9	84.6	93.1	97.1	99.0	99.7	100.0		

Unit of Probability : %
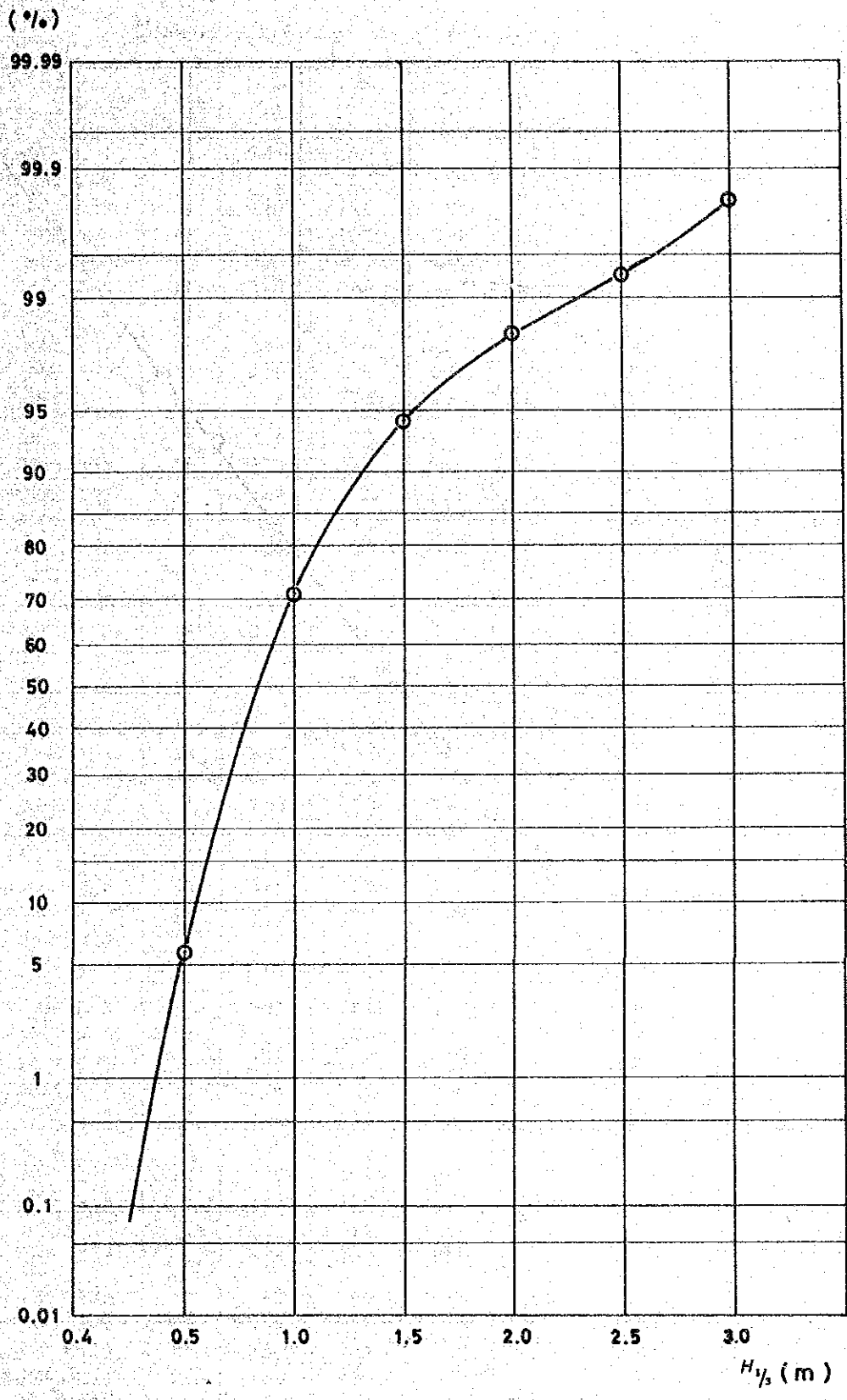
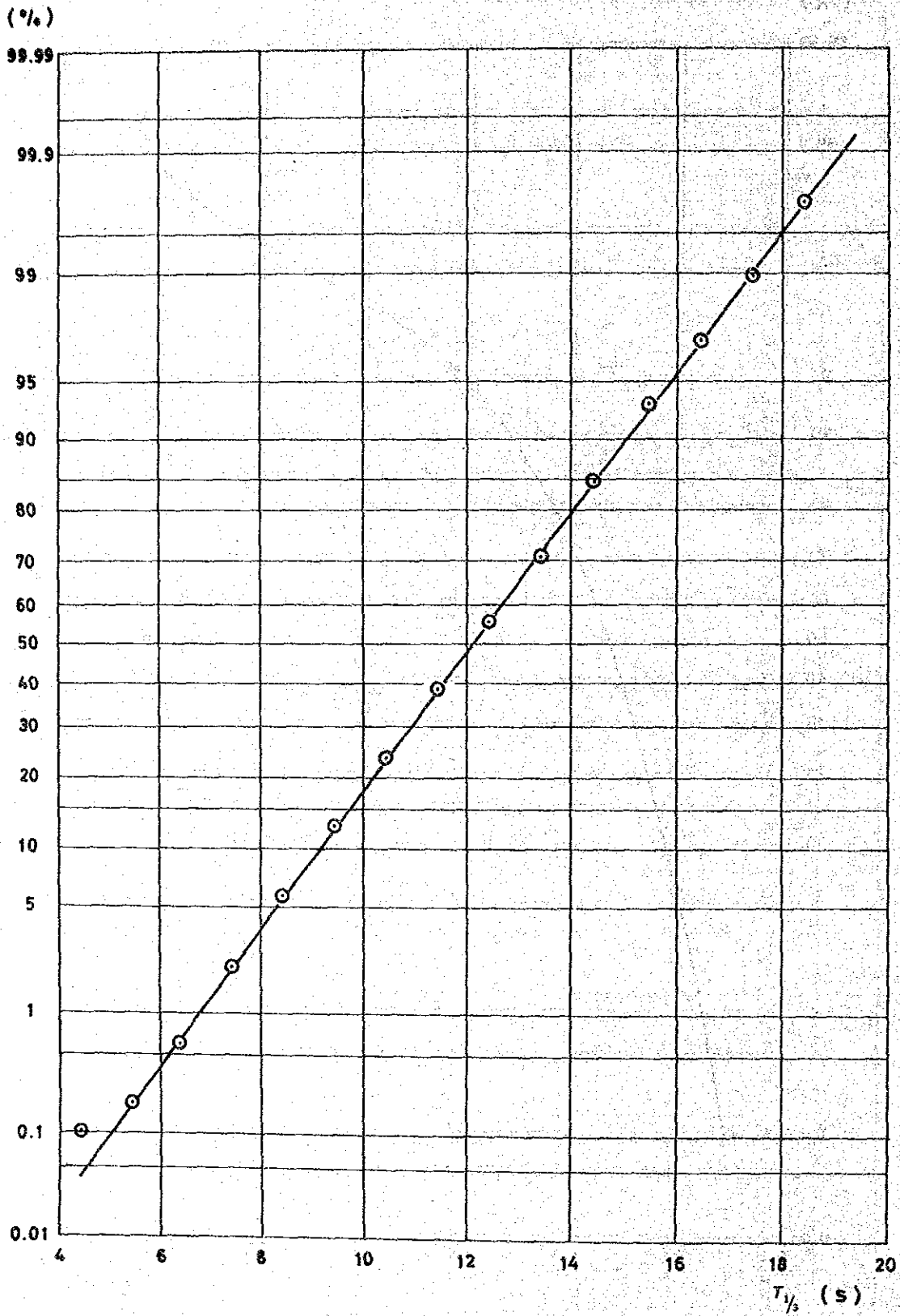Fig. IV-10 Cumulative Occurrence Probability of Significant Wave Height

Fig. IV-11 Cumulative Occurrence Probability of Significant Wave Period

Table IV-5 Record of Observed Wave Heights above 1.5m

Rank	Date of Observation	Time	H_{max} (m)	T_{max} (s)	$H_{1/10}$ (m)	$T_{1/10}$ (s)	$H_{1/3}$ (m)	$T_{1/3}$ (s)	H_{mean} (m)	T_{mean} (s)
1	1981. 5.21	16	5.44	16.9	4.17	17.8	3.55	17.9	2.19	15.1
2	1983. 7.18	4	4.44	16.8	4.09	17.2	3.47	17.1	2.31	16.1
3	1978. 6.18	8	4.10	18.0	3.90	17.8	3.30	17.5	1.90	15.0
4	1985. 5.28	17	4.17	16.3	3.74	17.7	2.94	17.8	1.85	15.5
5	1982. 3.18	12	3.83	15.7	3.10	16.1	2.86	15.9	1.33	12.3
6	1985. 9.13	17	3.66	19.8	3.47	17.7	2.77	17.6	1.73	13.0
7	1981. 5. 6	18	3.98	20.0	3.43	16.7	2.74	17.4	1.58	12.0
8	1983. 8. 7	24	3.80	16.9	3.27	17.3	2.66	17.5	1.71	16.0
9	1980.11. 5	8	3.36	17.7	2.95	17.6	2.53	17.1	1.55	12.5
10	1985.10. 2	23	3.22	17.6	2.83	17.3	2.49	17.0	1.54	12.3
11	1981.11.29	2	3.14	17.5	2.93	16.4	2.44	16.4	1.50	13.9
12	1980.10.16	22	3.55	18.1	3.11	17.3	2.22	17.1	1.30	12.4
13	1985.10.27	7	2.92	17.5	2.75	17.1	2.20	17.3	1.33	14.5
14	1982. 6.12	4	2.75	13.9	2.53	14.5	2.13	15.7	1.38	12.8
15	1978. 9.18	4	3.20	9.0	2.70	8.6	2.10	8.9		
16	1985. 5.17	18	3.05	16.9	2.55	17.3	2.10	16.1	1.26	10.7
17	1981.11.20	24	3.10	16.1	2.37	15.5	2.06	15.9	1.41	13.9
18	1985. 8.18	8	2.88	14.2	2.56	15.6	2.06	15.6	1.26	12.9
19	1981. 7.10	20	2.69	17.6	2.30	14.6	2.02	15.4	1.21	11.0
20	1978.10. 3	16	3.00	15.0	2.50	16.0	2.00	16.0		
21	1979. 8. 7	16	2.50	20.0	2.30	19.0	2.00	18.2	1.40	16.2
22	1981. 3.21	18	2.48	14.3	2.29	15.5	2.00	15.7	1.21	13.0
23	1981.11. 1	20	2.99	16.3	2.40	16.4	1.99	16.1	1.23	18.3
24	1978. 8. 6	4	3.20	14.0	2.40	14.5	1.90	14.5		
25	1979. 5.20	24	2.50	17.0	2.30	16.0	1.90	16.0	1.30	15.0
26	1985. 4.17	15	3.00	12.9	2.41	9.6	1.88	12.3	1.08	8.5
27	1985. 9.26	9	2.48	15.7	2.30	16.3	1.85	16.3	1.13	13.4
28	1985. 6.30	13	2.50	14.3	2.18	12.1	1.81	12.7	1.12	8.5
29	1979. 9. 7	16	2.70	18.0	2.30	16.0	1.80	15.4	1.10	12.2
30	1982. 8. 7	18	2.62	16.0	2.26	16.2	1.79	16.5	1.06	11.8
31	1985. 8. 5	11	2.45	17.8	2.17	16.3	1.75	16.5	1.16	13.7
32	1985. 3.19	2	2.53	16.0	2.12	17.0	1.74	16.7	1.16	13.7
33	1979. 9.25	16	2.50	16.0	2.10	16.0	1.70	15.0	1.20	12.0
34	1985. 9. 8	15	2.46	15.0	2.04	14.3	1.70	14.5	1.07	12.2
35	1981. 1.17	6	2.26	13.8	1.98	13.9	1.67	14.2	1.01	13.0
36	1982. 3. 9	14	2.35	14.3	2.03	13.7	1.61	13.5	0.96	9.7
37	1978. 9.12	20	2.70	14.0	2.00	15.4	1.60	15.0		
38	1983. 9. 9	6	2.45	15.6	1.98	14.9	1.60	15.0	1.01	11.4
39	1978. 7. 9	16	2.00	16.0	1.90	15.9	1.60	16.0		
40	1985. 7.17	4	1.93	16.0	1.80	15.7	1.58	16.1	1.06	14.0
41	1982. 5.19	10	2.42	14.9	1.93	14.9	1.57	14.8	1.00	12.5
42	1981. 2. 7	22	2.40	14.3	1.96	14.2	1.57	14.3	0.97	13.1
43	1982. 8.15	6	2.55	15.8	1.99	15.2	1.56	15.5	1.00	11.9
44	1984. 2.26	22	1.89	13.4	1.59	14.7	1.56	11.3	0.90	9.5
45	1985. 6.15	7	2.29	13.1	2.04	13.3	1.51	13.3	0.91	11.6
46	1983. 8.15	22	2.12	12.8	1.90	13.7	1.51	13.7	0.93	9.9
47	1980. 9.11	22	2.06	11.5	1.82	11.8	1.51	11.7	0.97	9.7
48	1978.10.15	4	1.90	16.0	1.70	15.0	1.50	14.0		

Table IV-6 Probable Wave Heights Corresponding to Respective Recurrence Periods

Recurrence Period (Years)	Significant Wave Height $H_{1/3}$ (m)	Significant Wave Period $T_{1/3}$ (m)
5	3.692	17.97
10	3.980	18.26
20	4.259	18.50
25	4.348	18.57
30	4.419	18.62
40	4.531	18.71
50	4.617	18.78
100	4.881	18.97
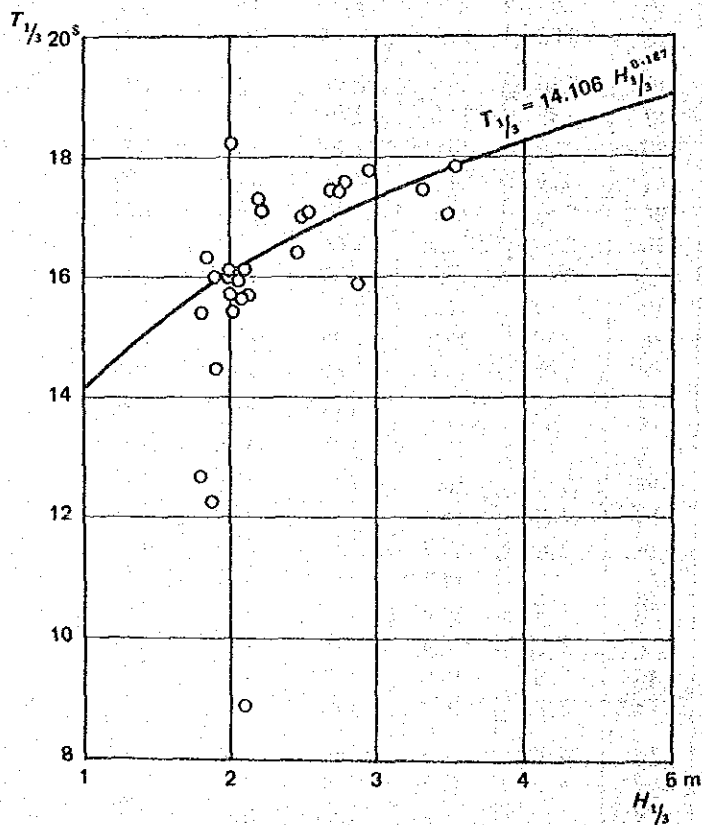
Fig. IV-12 Relationship between Significant Wave Height and Significant Wave Period of Extremely Large Waves

The significant wave period of each probable wave shown in Table IV—5 is, as shown in Fig. IV—12, estimated from the relationship between the significant wave height and the significant wave period of extremely large waves.

3. 2 Direction of Wave Incidence and Wave Refraction Coefficients in the Port of Caldera Area

In order to find the direction of wave incidence and the wave refraction coefficients in the Port of Caldera area, refraction calculations were carried out as part of the Feasibility Study on the Second Stage Expansion Project of the Port of Caldera performed in 1981.[4] The refraction calculations were carried out using the orthogonal method, and, as stated above, the waves in this sea area are believed to exhibit behaviour similar to regular waves. Hence for the purposes of calculation, the waves are assumed to be regular waves. A refraction calculation was first performed north of lat. 9°36′N. in a rectangular sea area with a north-south dimension of 40 km and an east-west dimension of 50 km. Then, a greatly reduced refraction chart was prepared for an area to the north side of the parallel passing through the southern edge of Icaco Beach south of Cape Carralillo. The prepared refraction chart is shown in APPENDIX 1.

The refraction coefficients and wave directions along the parallel of latitude passing through the southern edge of Icaco Beach south of Cape Corralillo are shown in Table IV—7 and Table IV—8. The direction of wave incidence near the tip of the Port of Caldera breakwater is shown in Table IV—9. Despite their having deep water wave directions and periods, the direction of waves incident to the tip area of the Port of Caldera breakwater are, with little variation, between N 220° to 230°.

3. 3 Tidal Conditions

Simple water pressure type tide measurements were performed at the roll—on/roll—off pier at the Port of Caldera between October 8 and November 15, 1985. A harmonic analysis was performed using data obtained on the 15 days and nights from midnight October 17, 1985 to 11 PM October 31. The obtained harmonic constants of a principal ten component tide are shown in Table IV—10. The tidal constant of the Port of Puntarenas [5] is also noted in the table. According to the table, the harmonic constants of the two ports are similar, and the tidal fluctuations are roughly the same. At both ports, a half-day periodic component prevails. The single day periodic component is minute. According to the tide table of the British Navy, the seasonal mean water level fluctuation in October is 0.0 m; hence it is likely that the mean water level at the time of the observations was virtually the same as the annual mean water level.

---

4) Japan International Cooperation Agency: The Feasibility Study on the Second Stage Expansion Project of the Port of Caldera, Republic of Coast Rica, Dec. 1981, 343 p.
5) Hydrographer of the Navy (G.B.); Admiralty Tide Table, Vol. 3, Pacific Ocean Ed., 1980, 452 p.

Table IV-7 Refraction Co-efficient along the Parallel of Latitude Passing through the Southern Edge of the Icaco Beach

Wave Direction Wave Period (s)	157.5° S S E	180.0° S	191.3°	202.5° S S W	213.8°	225.0° S W
8	—	0.87	1.00	0.84	0.67	0.33
10	0.30	1.00	1.00	0.82	0.42	0.16
12	0.40	0.91	0.80	0.88	0.35	< 0.15
14	0.55	0.88	0.60	0.79	0.25	< 0.15
16	0.65	0.84	0.83	0.75	0.20	< 0.15
18	0.70	1.34	1.33	0.77	0.17	< 0.15
20	0.30	1.27	1.41	0.75	0.15	< 0.15

Source : JICA

Table IV-8 Wave Direction along the Parallel of Latitude Passing through the Southern Edge of the Icaco Beach

Wave Direction Wave Period (s)	157.5° S S E	180.0° S	191.3°	202.5° S S W	213.8°	225.0° S W
8	—	182°	193°	205°	216°	—
10	—	183°	195°	208°	217°	—
12	—	185°	196°	210°	217°	—
14	—	186°	198°	211°	217°	—
16	—	189°	199°	212°	218°	—
18	—	191°	202°	214°	219°	—
20	—	193°	204°	215°	219°	—

Source : JICA

Table IV-9 Incident Wave Direction at the Port of Caldera

Wave Direction Wave Period (s)	191.3°	202.5° S S W
12	220°	224°
16	223°	228°
20	225°	229°

Source : JICA

Fig. IV-13 was calculated according to the amplitude of a principal four tidal constituent in Table IV-10, and shows the principal tide levels at the Port of Caldera and the Port of Puntarenas. The tidal ranges of the two ports are compared in Table IV-11. Each tidal range at the Port of Puntarenas is 11 to 19 cm greater. However, the values for the Port of Caldera are based on observation data taken over a 15 day period, and hence it is not clear how significant the differences are. It may be safer to assume that there are only negligible differences.

Table IV-10 Harmonic Constants of Tides

(1985.10.17~31)

Tidal Constituent	Caldera			Puntarenas		
	Amp.	Lag		Amp.	Lag	
	H (m)	k (°)	g (°)	H (m)	k (°)	g (°)
M_2	1.025	80.3	75.8	1.10	76.5	72
S_2	0.270	136.1	125.5	0.25	136.6	126
K_2	0.047	136.1	125.5			
N_2	0.211	64.1	62.9			
K_1	0.087	342.4	336.9	0.10	349.5	344
O_1	0.045	14.8	15.8	0.04	22.9	24
P_1	0.029	342.4	337.4			
Q_1	0.023	45.5	49.8			
M_4	0.011	180.9	171.9			
MS_4	0.008	301.3	286.3			
A_0	1.496					

Note 1) The latitude and longitude of each port are,
   Caldera : N 9° 54' 42", W84° 43' 1"
   Puntarenas : N 9° 58', W84° 50'
2) In the Lag column,
   k indicates Costa Rican time standard
   g indicates Greenwich standard

Table IV-11 Tidal Range at Caldera and Puntarenas

	Caldera	Puntarenas
Large Tidal Range (m)	2.590	2.70
Mean Tidal Range (m)	2.050	2.20
Small Tidal Range (m)	1.510	1.70

(1) Caldera		(2) Puntarenas	
N.H.H.W.L.	+1.427	N.H.H.W.L.	+1.49
H.W.O.S.T.	+1.295	H.W.O.S.T	+1.35
M.H.H.W.	+1.118	M.H.H.W.	+1.20
M.H.W.	+1.025	M.H.W.	+1.10
H.W.O.N.T.	+0.755	H.W.O.N.T	+0.85
M.S.L.	±0.000	M.S.L.	±0.00
L.W.O.N.T.	−0.755	L.W.O.N.T.	−0.85
M.L.W.	−1.025	M.L.W.	−1.10
M.L.L.W.	−1.118	M.L.L.W.	−1.20
L.W.O.S.T.	−1.295	L.W.O.S.T.	−1.35
N.L.L.W.L.	−1.427	N.L.L.W.L.	−1.49
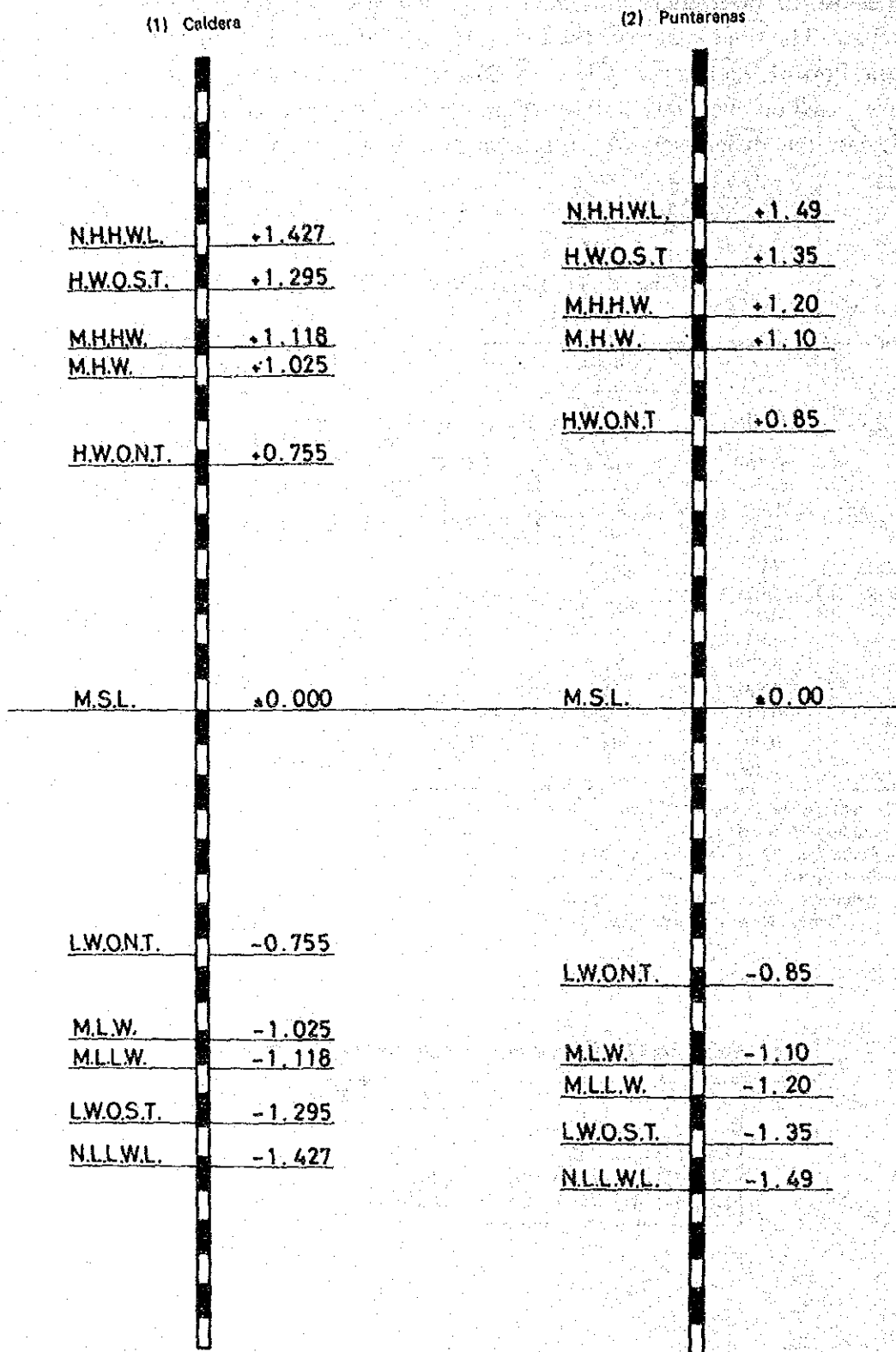
Fig. IV-13   Tide Levels at Caldera and Puntarenas

3.4 Current

Current observation was performed by JST in cooperation with MOPT at the Port of Caldera and the surroundings area between October 9 and November 8, 1985, for the purpose of understanding the local sand drift phenomenon. Current observation comprised round the clock fixed point observations (4 locations) over 15 days using an Ono—type current meter, and double tide and single tide observations (15 locations) performed by a CM—2 D current meter for interpolating the above observations. The details of current observations and their results are shown in APPENDIX 3.

Fig. IV—14 and Fig. IV—15 shows current distribution during maximum northward and southward currents.

According to these figures, northward current during flood and southward current during ebb prevail in the offshore area of the Port of Caldera. The maximum current velocity is approximately 22 cm/s offshore of the New Beach. On the other hand, in the harbour area, a clockwise current always prevails. In this area, maximum velocity is approximately 7 cm/s during ebb.

3.5 Sand Drift

Depth sounding, shoreline measuring, sediment sampling and analysis, fluorescent sand analysis, and a sectional study at the mouth of the Mata de Limón Estuary were performed between October 9 and November 7, 1985 at the Port of Caldera and the surrounding shoreline and sea area for the purpose of understanding the local sand drift phenomenon. The details of these studies and their results are shown in CHAPTER VI.

ST. 0-2
12.8

ST. 0-3
14.2

ST. 0-4
1.6

ST. 0-1
20.4

CALDERA
Time: 1 Hour After Low Water
(Unit: cm/s)

0   500 m
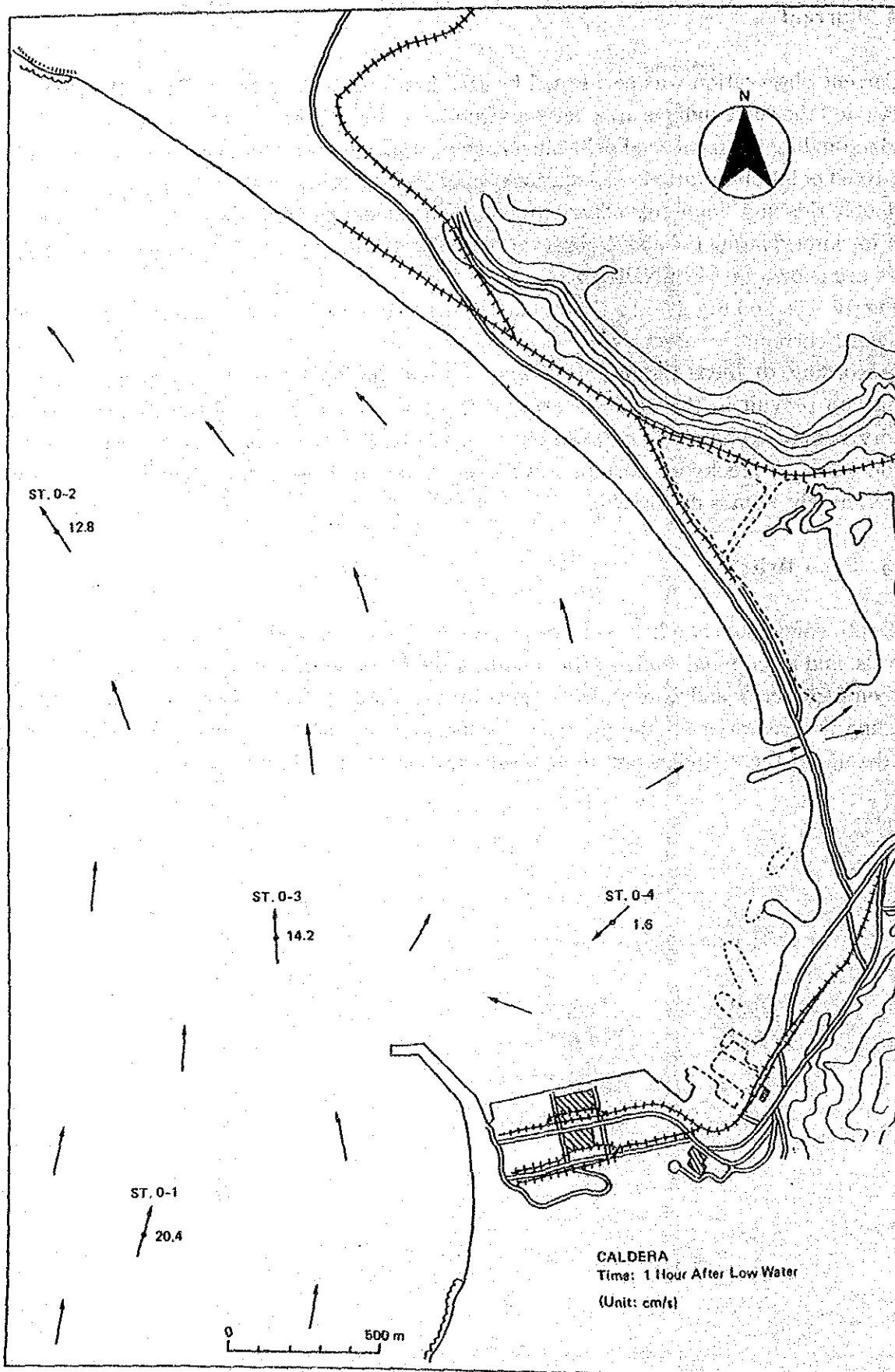
Fig. IV-14   Mean Current Distribution at Spring Tide (Northward Current)

ST. 0-2
• 12.7

ST. 0-3
↓ 15.3

ST. 0-4
↓ 6.6

ST. 0-1
↓ 22.4

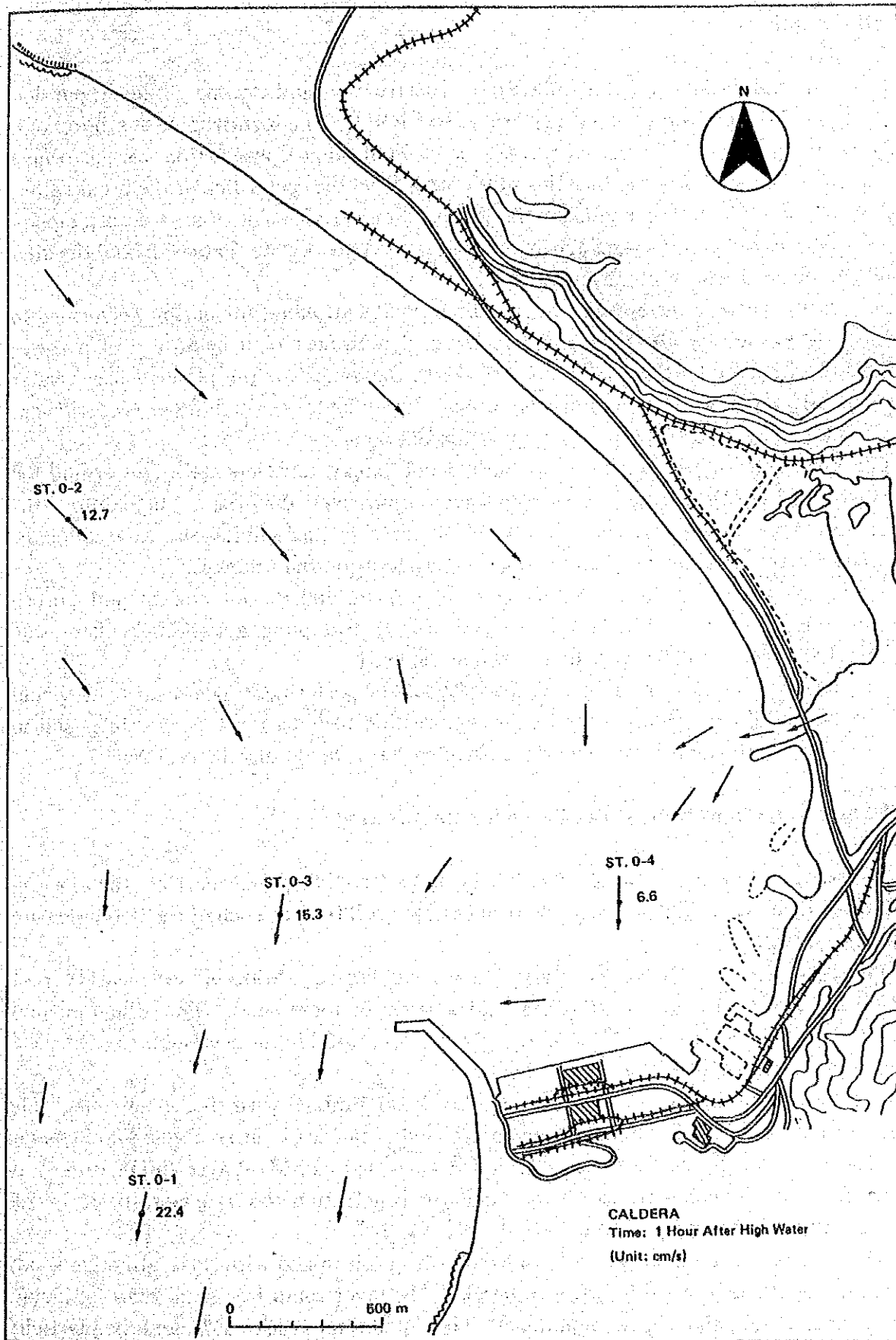CALDERA
Time: 1 Hour After High Water
(Unit: cm/s)

N

0 ⌐ 500 m

Fig. IV-15 Mean Current Distribution at Spring Tide (Southward Current)

4. Soil Conditions

The soil explorations for the First Stage Construction and Second Stage Expansion Project of the Port of Caldera were performed by MOPT. The locations of the boreholes are shown in Fig. IV-16. The boring carried out for First Stage Construction was performed principally in the vicinity of the face line of the wharf and the center line of the breakwater. The boring carried out to consolidate the Second Stage Expansion Plan was principally performed in the vicinity of the center line of the planned breakwater extension and the area around the planned wharf expansion zone.

Boring was carried out by the wash method. Sea scaffolding for boring performed in relation to consolidating the Second Stage Expansion Project plan made use of a tower constructed of steel tubing with attached floats in the zones for the planned breakwater extension, and pontoons were used in other areas. Sampling for the soil test was carried out using a BX Shelby tube (open sampler of 50 mm diameter).

The above mentioned soil investigation did not supply sufficient data concerning the shearing strength of the cohesive layer, and some samples were disturbed. Furthermore, the coefficient of consolidation was not reported. Therefore, further soil investigation should be performed for the detailed design, taking into consideration the following.

a) The interval of boreholes should be 25 m to 50 m, and the interval of undisturbed sampling depth should be less than 1.5 m. For the sampling, a stationary piston thin wall sampler with 75 mm diameter should be used.

b) Laboratory soil tests, mainly shear tests, should be performed. The shear tests should be unconsolidated-undrained triaxial compression tests as much as possible, and in addition to the above consolidated-undrained tests should also be performed.
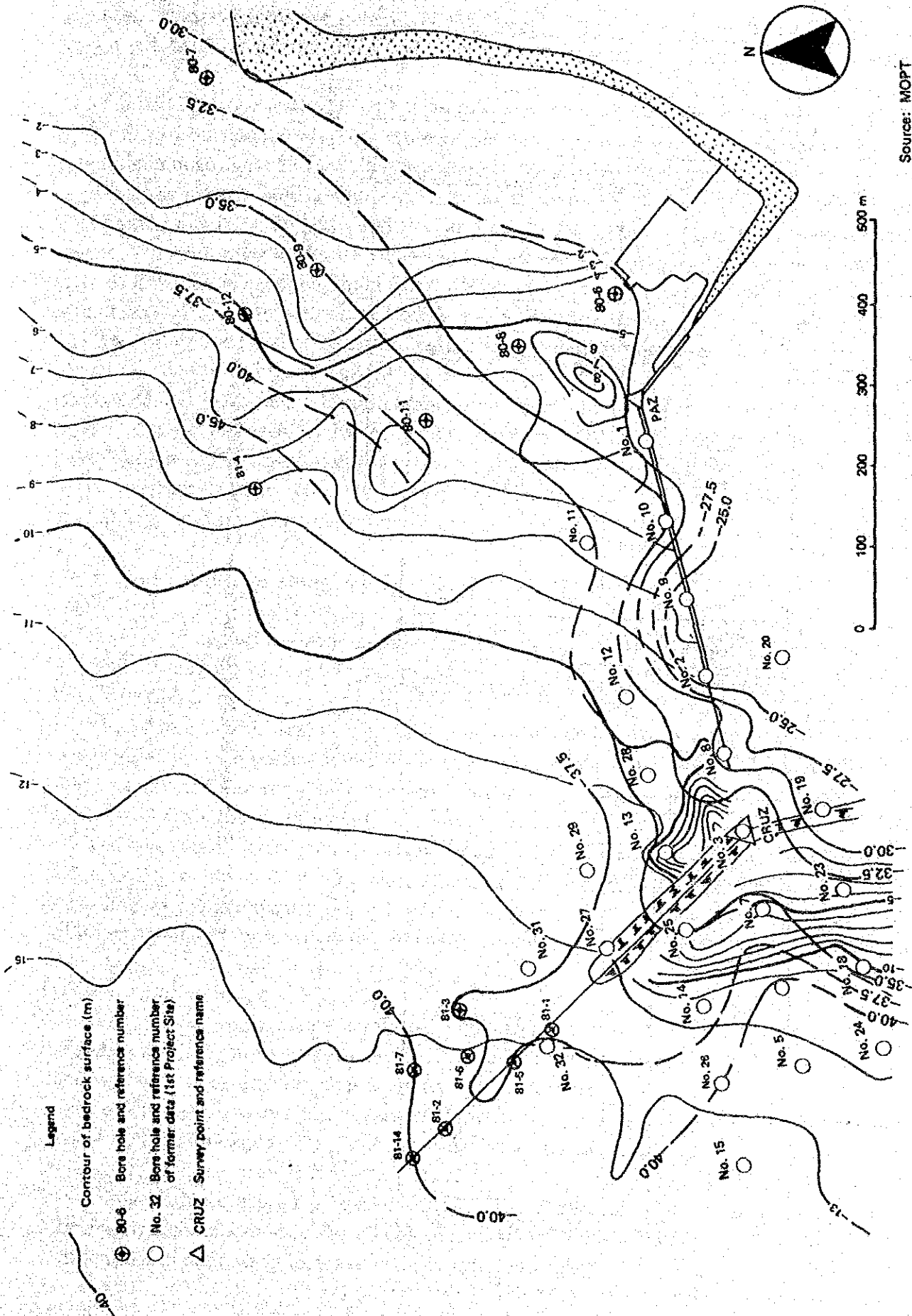
4.1 Soil Conditions around the Extended Breakwater

An estimated soil profile at the extended center line of the trunk part of the existing breakwater is shown in Fig. IV-17. The results of the soil tests at each of the boreholes are shown in APPENDIX 2.

The submarine soil strata comprise a layer of Tertiary Miocene sedimentary rock covered by deposited cohesive alluvium, and a layer of loose sand. This alluvium may generally be divided into three layers, namely Sa, Mb, and Mc, in descending order. The characteristics of each layer are given below.

The Sa bed consists of fine to very fine black sand mixed with shell fragments. The lower portion of the bed becomes silty in nature, and occasionally intercalates thin layers of silt. The sand content of Sa is 5to40% and is classified as SM. Layer thickness is 7 to 10 meters. The N value based on the standard penetration test is generally 10 to 20, however silty areas may drop to below 10.

The Mb layer consists principally of sandy silt or silt mixed with sand, although sandy layers are occasionaly found interposed therein. The layer comprises sand, 20 to 40%, clay, approximately 20%, and silt, the remainder. The liquid limit is 40 to 55%, and the plasticity index is 10 to 20, which means the plasticity is slightly low. The soil is classified as ML, CH,
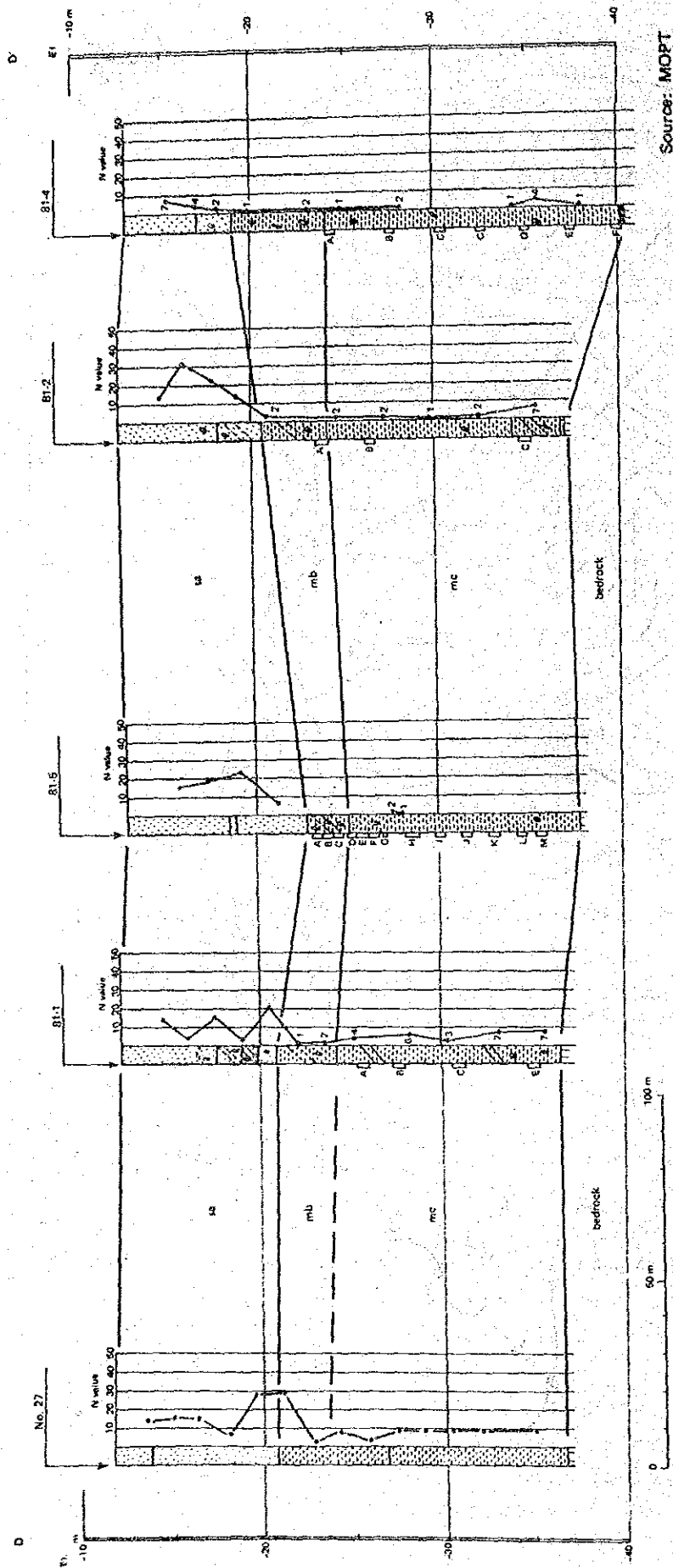
Fig. IV-16　Map of Borehole Locations

Source: MOPT

Fig. IV-17   Estimated Soil Profile around the Extended Breakwater

Source: MOPT

and MH. Natural moisture content is 47% to 57% which is near the liquid limit. Unit weight is 1.66 to 1.74 tf/m³. The layer has a thickness of 2.5 to 7 meters, and an N value of 1 to 4.

The Mc layer is mostly silt with a small amount of shell fragments. The lowest portion of the layer occasionaly interposes thin gravelly layers mixed with silt. In addition to silt, texture composition is 2 to 15% sand, and 10 to 30% clay. The upper portion of the layer has a slightly greater sand component, while the lower portion has a greater clay component. The liquid limit is 52 to 62%, and the plasticity index is 20 to 30, which means that the plasticity is somewhat moderate. The soil is classified as MH. Natural moisture content is 48 to 57% which is near the liquid limit. Unit weight is 1.68 to 1.74 tf/m³. The layer has a thickness of 10 to 16 meters, and an N value of 1 to 7.

The unconfined compression strength and unit weight of the Mb and Mc layers are plotted by depth in Fig. IV—18. Fig. IV—19 shows a plot of cohesion according to an unconsolidated undrained triaxial compression test. The cohesion of the Mb and the Mc layer is 4 tf/m² at the top edge of the layer, and 8 tf/m² at the bottom of the layer. A consolidation test was performed, though only the consolidation yield stress and compression index results were reported. The consolidation yield stress was reported as being 1.3 to 1.7 kgf/cm², and the compression index as 0.43 to 0.47.

4. 2 Soil Conditions along the Face Line of the Wharf

Fig. IV—20 shows the estimated soil profile along the face line of the wharf which is based on an examination of the soil conditions carried out during the planning of the First Stage Construction.

The submarine soil strata in this area comprise a layer of Tertiary Miocene sedimentary rock covered by a deposit of cohesive alluvium, and a layer of loosesand. This alluvial layer can be subdivided into three layers, a top sandy layer, a cohesive layer, and a bottom sandy layer, the characteristics of each of which are explained below.

The top sandy layer comprises rough and fine sand, and has a thickness of 7 to 15 meters which narrows as it approaches the western side, i.e. the breakwater foundation. According to the standard penetration test, the N value is generally between 20 and 50, with a variable density in which dense portions are numerous. However, there are instances where the value drops to 10 in parts of the surface layer and in the silty portions. This layer is classified as S, SW, and SP.

The cohesive layer comprises largely homogenous, slightly hard silt, and is thicker towards the west. On its eastern side, that is, in the −7.5 m quay area, it is 2 to 4 meters thick, and on its western side, that is, in the −11 m quay area, it is 3 to 11 meters thick. The soil in this layer is mostly classified as ML, however portions of MH and CH are also found. The N value is mostly 4 to 15, though it becomes smaller towards the west. At the edge of the −11 m quay area it becomes 3 to 7 across all layers. Fig. IV—21 shows a plot (according to depth using the seabed surface as a standard) of the shear strength of this cohesive stratum based on the results of an unconfined compression test. Shear strengths at identical depths and their increase ratio in relation to depth have similar values along the

Total Unit Density
γ (t/m^3)

1.6   1.7   1.8

Unconfined Compression Strength
q_u (t/m^2)

0   5   10   15   20

Elevation in m

-15

◇ 81-1
▽ 81-2
□ 81-3
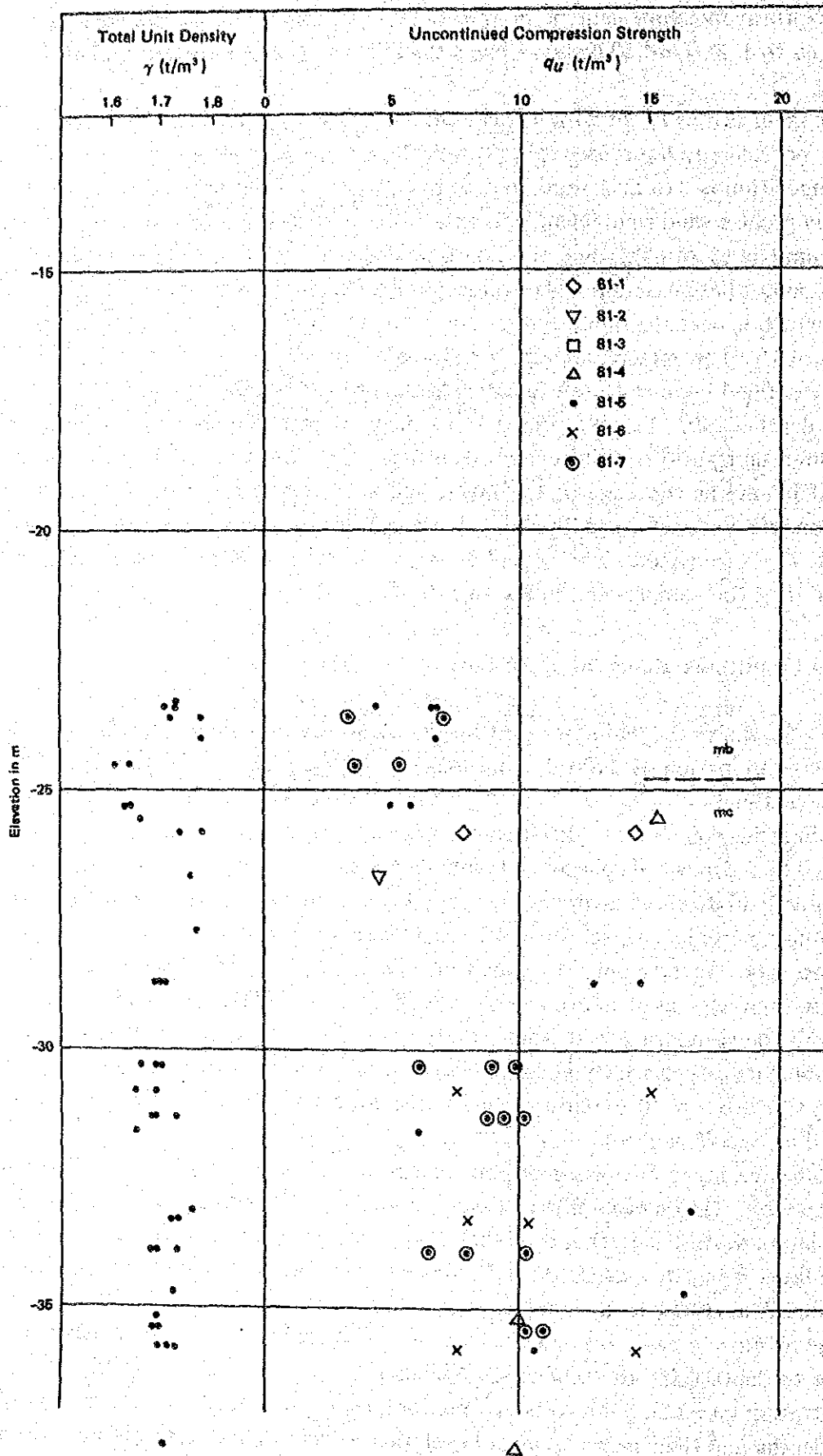△ 81-4
• 81-5
✕ 81-6
◉ 81-7

-20

mb

mc

-25

-30

-35

Fig. IV-18   Unit Weight and Unconfined Compression Strength of the Cohesive Layer
around the Extended Breakwater

Total Unit Density γ (t/m³)
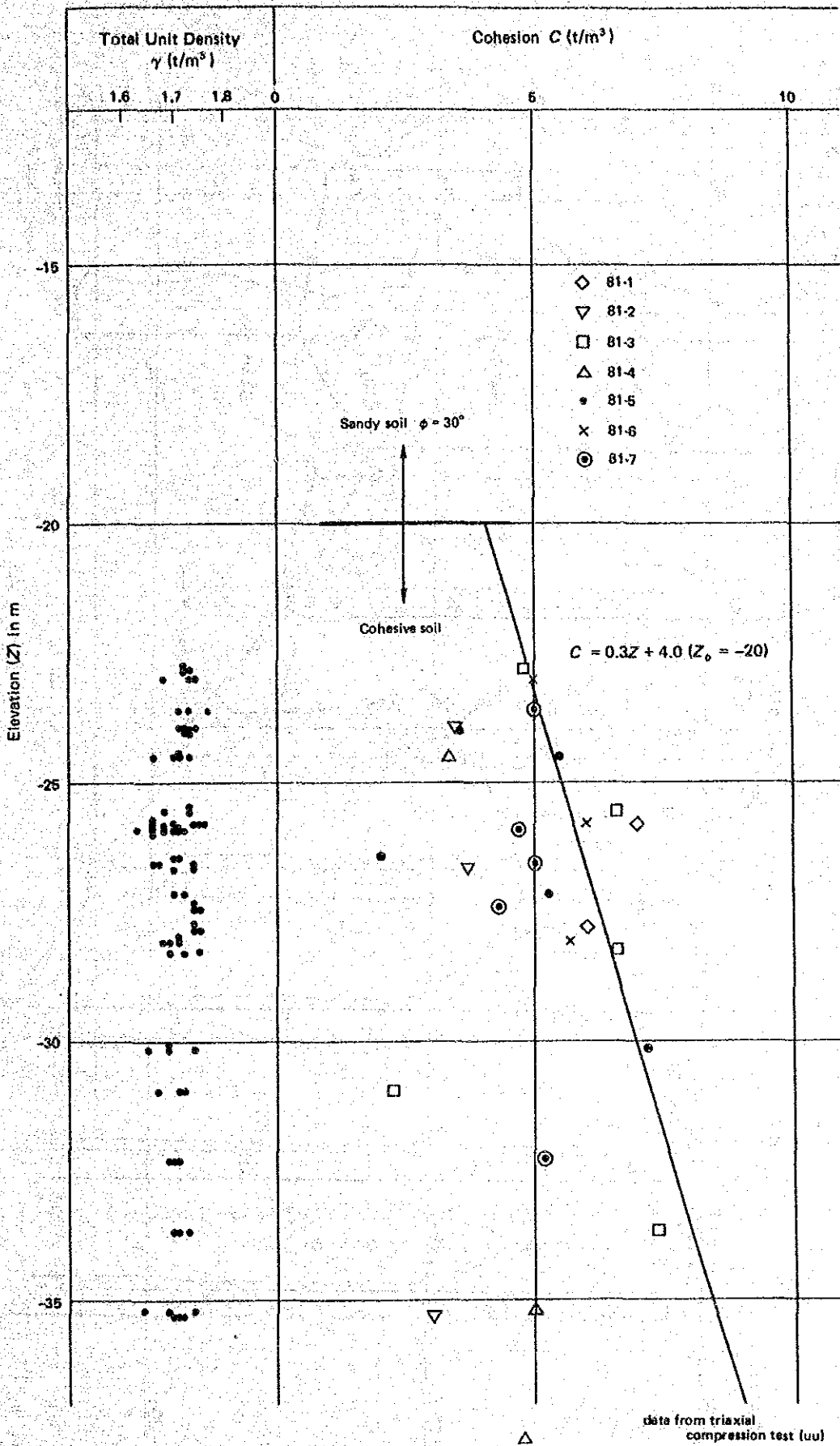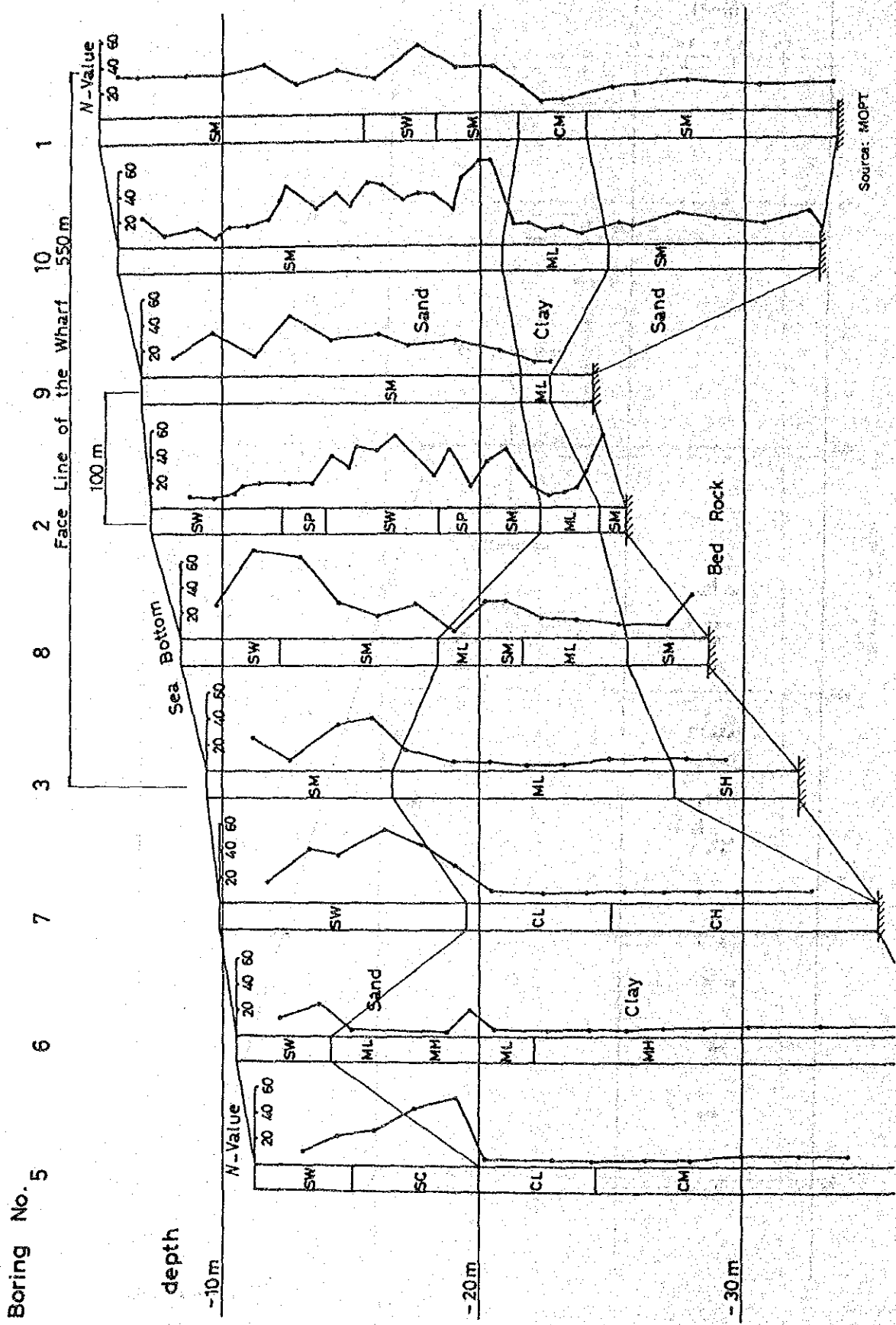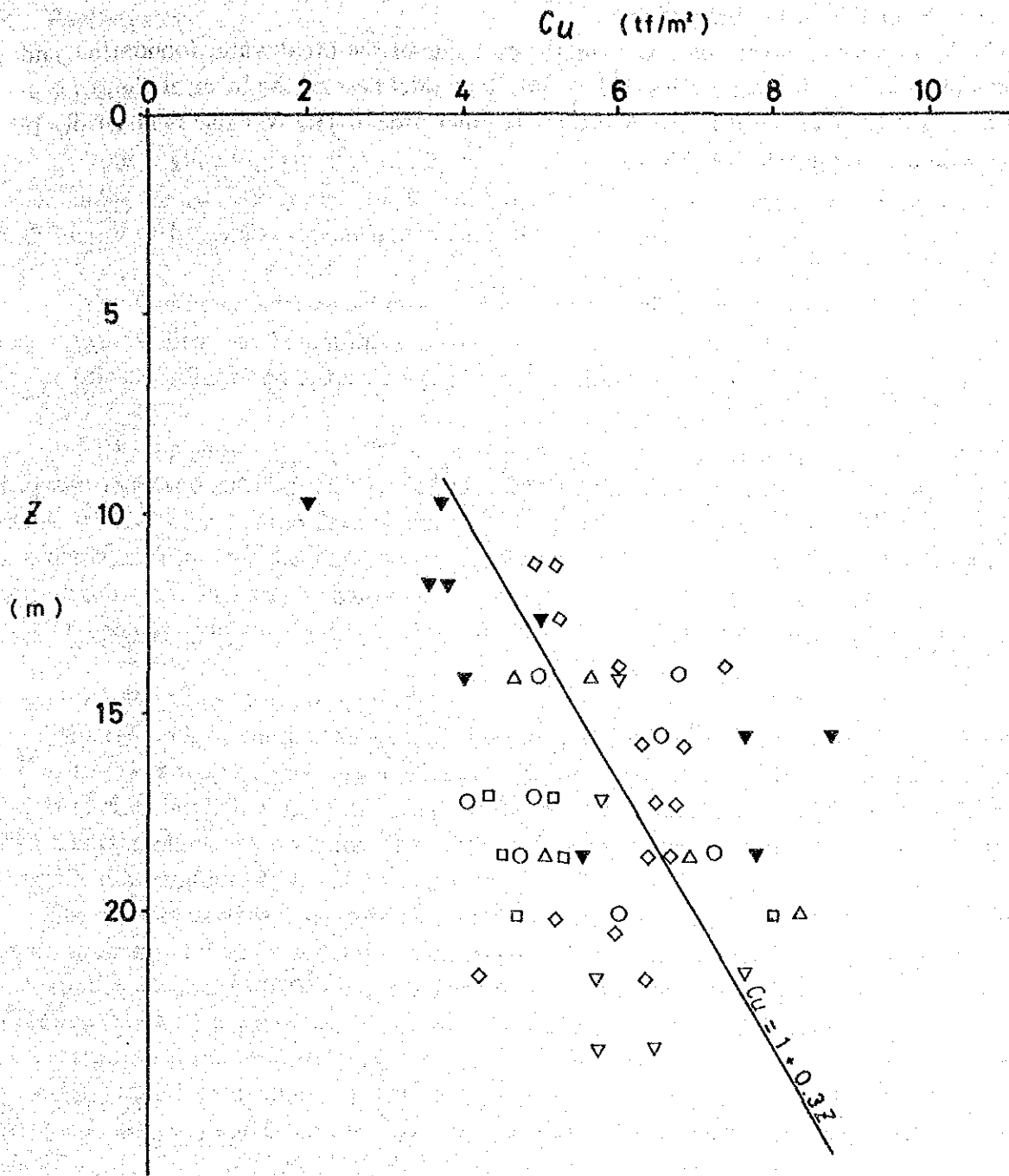
1.6 1.7 1.8

Cohesion C (t/m³)

0   5   10

◇ 81-1
▽ 81-2
□ 81-3
△ 81-4
• 81-5
× 81-6
◉ 81-7

Sandy soil $\phi = 30°$

Cohesive soil

$C = 0.3Z + 4.0\ (Z_0 = -20)$

Elevation (Z) in m

data from triaxial
compression test (uu)

Fig. IV-19 Cohesion of the Cohesive Layer around the Extended
Breakwater according to a Triaxial UU-Test

Fig. IV-20   Estimated Soil Profile along the Face Line of the Wharf

Fig. IV-21 Cohesion of the Cohesive Layer along the Face Line of the
Wharf according to an Unconfined Compression Test

extended center line of the breakwater.

The bottom sandy layer only exists on the east side of the breakwater foundation, and consists of sand and silty sand classified as SM. The thickness of the layer at the -7.5 m quay area is 8 to 10 m and it is 1 to 5 m thick in other areas. The N value is generally 10 to 20, with a medium relative density.

5. Earthquakes

5. 1 Earthquake Activity in Costa Rica

As indicated by Fig. IV-22, Costa Rica may be divided into three regions based on past earthquake records and a geological study relating to the development mechanics, magnitude, depth of focus and topographic distribution as follows [6].

(1) Pacific Coast Border Region
(2) Valley and Mountain Region
(3) Northern and Atlantic Coast Plain Region

Fig. IV-22 shows the locations of epicenters and origins of earthquakes occuring between 1888 and 1983 which were of considerable intensity or caused significant damage. Table IV-12 indicates the date of occurence, the region, the magnitude and a summary of the damage from all the earthquakes occuring between 1756 and 1983 which were of considerable size or caused significant damage.

The characteristics of earthquake activity in the three regions are explained below.

(1) Pacific Coast Border Region
This region is vulnerable to earthquakes caused by the subduction of the Carib Plate on which the Costa Rican territory is situated by the Cocos Plate of the Pacific sea bottom which is creeping below the Carib Plate offshore at the Pacific Central American Trench. These earthquakes move inland, and accordingly are charactrerized by deepening focuses, the maximum values of which reach 200 km.

The scale of earthquakes caused by subduction of the plate is potentially very great, and an earthquake of 7.75 in magnitude was recorded in 1904. As a result, the energy of these earthquakes accounts for the major portion of the earthquake energy released in Costa Rica, although the resulting damage is not great. The reason for this is that although the depths of the focuses in the Pacific Coast. Region are undoubtedly comparatively shallow (20 km or more), they travel inland and their focuses deepen, hence the strength of the tremors become smaller. In general, the earthquakes in this region almost never exceed VII on the Modified Mercalli intensity scale. The Holy Saturday earthquake that occured on April 2, 1983 had an intensity in the central highlands of VI∼VII.

(2) Valley and Mountain Region
Earthquakes in this area are caused principally by localized faults. They are moderate in scale, with magnitudes of 6.5 or less. However, their focuses are shallow, and they occur close to areas of concentrated human population. Hence not only do tremors reach a powerful IX on the Modified Mercalli intensity scale, damage also increases due to addi-

---

6) Luis Diego Morales M.; Los Temblores, sus Causas, Medición y Efectos, Setiembre Cientifico, Vol. 2, Sep. 1985, pp. 43∼83
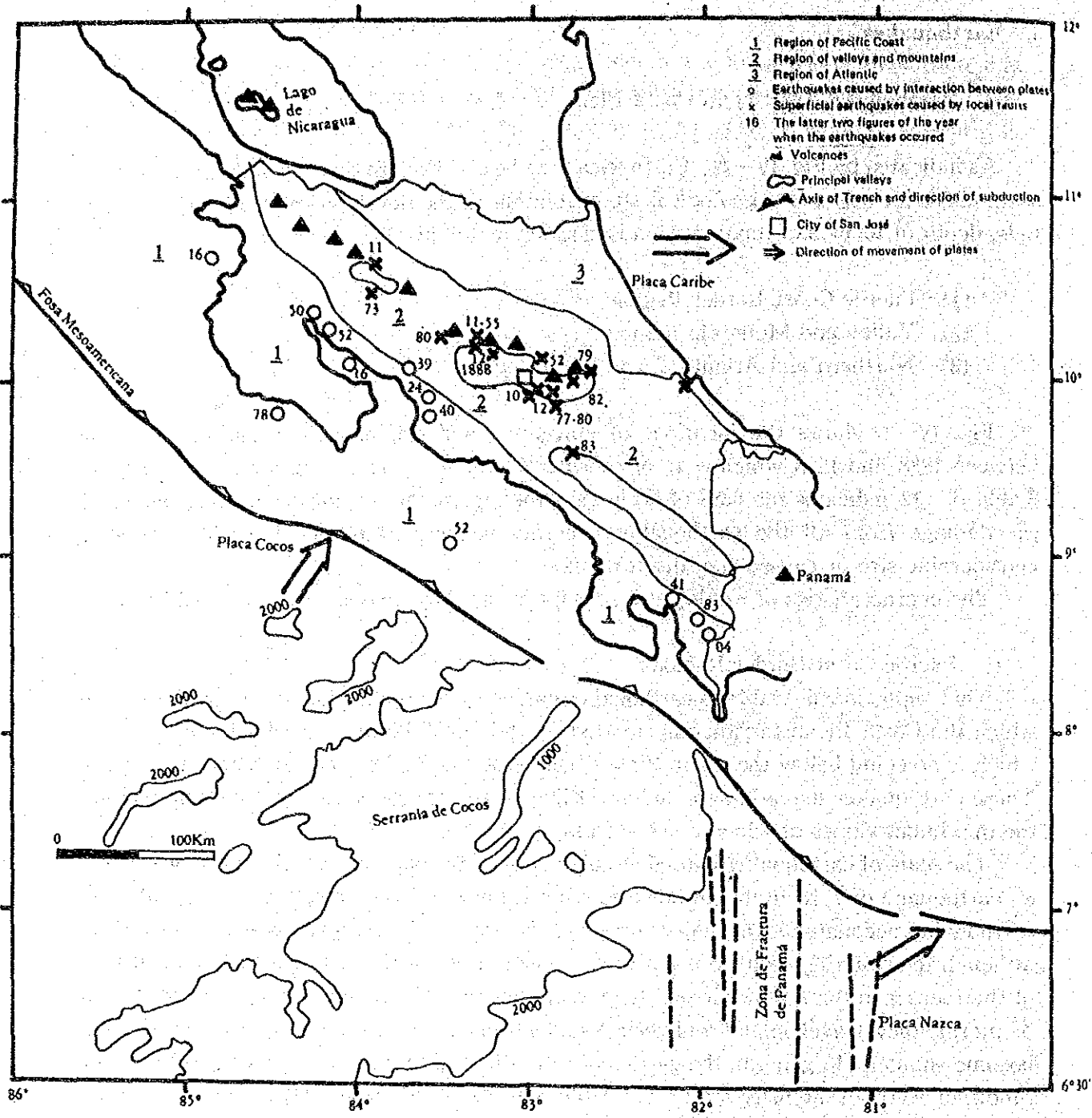
Fig. IV-22 Seismic Regions and Epicenters of Principal Earthquakes
which Occurred between 1888 ~ 1983 in Costa Rica

Table IV-12 Important Earthquakes which Occurred in Costa Rica *

Year	Date	Region	Magnitude	Coment
1756	14 Jul.	Earthquake of San Buenaventura (Epicentre is indefinite)	—	Damages in Cartago
1798	22 Feb.	Earthquake of Matina (Epicentre is indefinite)	—	
1822	7 May.	Earthquake of Matina (Epicentre is indefinite)	—	Damages throughout the region
1841	2 Sep.	Earthquake of Santa Mónica near Cartago	—	Primary destruction in Cartago
1851	18 Mar.	Strong earthquake near Alajuela	—	Damages in Alajuela and San José
1888	30 Dec.	Earthquake of Fraijanes	—	Damages in Alajuela and San José, Lake of Fraijanes created
1904	20 Dec.	Strong earthquake near the Panamá border	7.75	No damage was reported
1910	13 Apr.	Earthquake of Tablazo	<5.5	Damages in San José
1910	4 May.	Earthquake of Cartago	≦5.5	Secondary destruction of Cartago, 362 dead.
1911	28 Aug.	Earthquake of Toro Amarillo	—	Moderate damages and landslides
1911	10 Oct.	Earthquake of Guatuso (north of Lake of Arenal)	* *	Landslides, cracks in the ground
1912	6 Jun.	Earthquake of Sarchí (hill of Palomo)	* *	Large damages, landslides and damming of river from debris.
1916	27 Feb.	Earthquake (near Playa del Coco in Golfo de Papagayo)	7.5	Damages in Sardinal and Santa Cruz
1924	4 Mar.	Earthquake of Orotina (San Mateo-San Ramón)	7.0	Violently shaked Central Valley, damages throughout the region
1939	21 Dec.	Strong earthquake, region of Golfo de Nicoya	7.3	No damage was reported
1941	5 Dec.	Strong earthquake near Golfito	7.5	No damage was reported
1950	5 Oct.	Earthquake of Guanacasute (mouth of Río Tempisque)	7.7	Damages in Puntarenas
1952	30 Dec.	Earthquake of Patillos (northwest slope of Volcán Irazú)	* *	21 dead in landslide
1953	7 Jan.	Earthquake of Limón	* *	Moderate damages in Limón
1955	1 Sep.	Earthquake of Toro Amarillo (Grecia)	* *	Damages in the Valley of Río Toro Amarillo
1973	14 Apr.	Earthquake of Tilarán	6.5	Damages in the region of Tilarán, 23 dead
1983	2 Apr.	Earthquake of Osa-Golfito	7.3	Moderate damages throughout the region including San José, 1 dead
1983	3 Jul.	Earthquake of Pérez Zeledón	6.1	Important damages in the northen region of San Isidro and moderate damages in San Isidro, 1 dead

* It is a partial list including only earthquakes which which were large or which caused significant damage.
* * Estimated magnitude is $5 \leqq M_s \leqq 6.5$.
Source : Luis Diego Morales M.

tional disasters caused by landslides and floods from damaged dams. Damage-causing earthquakes in Coast Rica occur principally in this region, and as shown in Fig. IV—22, and often originate invalley areas.

The Cartago earthquake which occured on May 4, 1910 caused the greatest level of earthguake damage. In more recent years, the Pérez Zeledón earthquake occured in this area on July 3, 1983 between Buena Vista and División which are located in the northern district of San Isidro.

(3) Northern and Atlantic Coast Plain Region

From the view point of techtonics, this is a quiet region in Costa Rica with little earthquake activity. The locations of earthquake occurances tend to be spread out (refer to Fig. IV—22). However, an earthquake with powerful tremors hit the City of Limón on January 7, 1953 and caused great damage.

5. 2 Distribution of Expected Seismic Acceleration Values

Fig. IV—23 and Fig. IV—24 show the distribution of expected ground acceleration values calculated for Costa Rica over a 50 year recurrence period and a 100 year recurrence period. The values are based on the record of past earthquakes occuring between 1883 and 1975 and were calculated by C. P. Mortgat, T. C. Zsutty, H. C. Shah, and L. Lubetkin.[7]
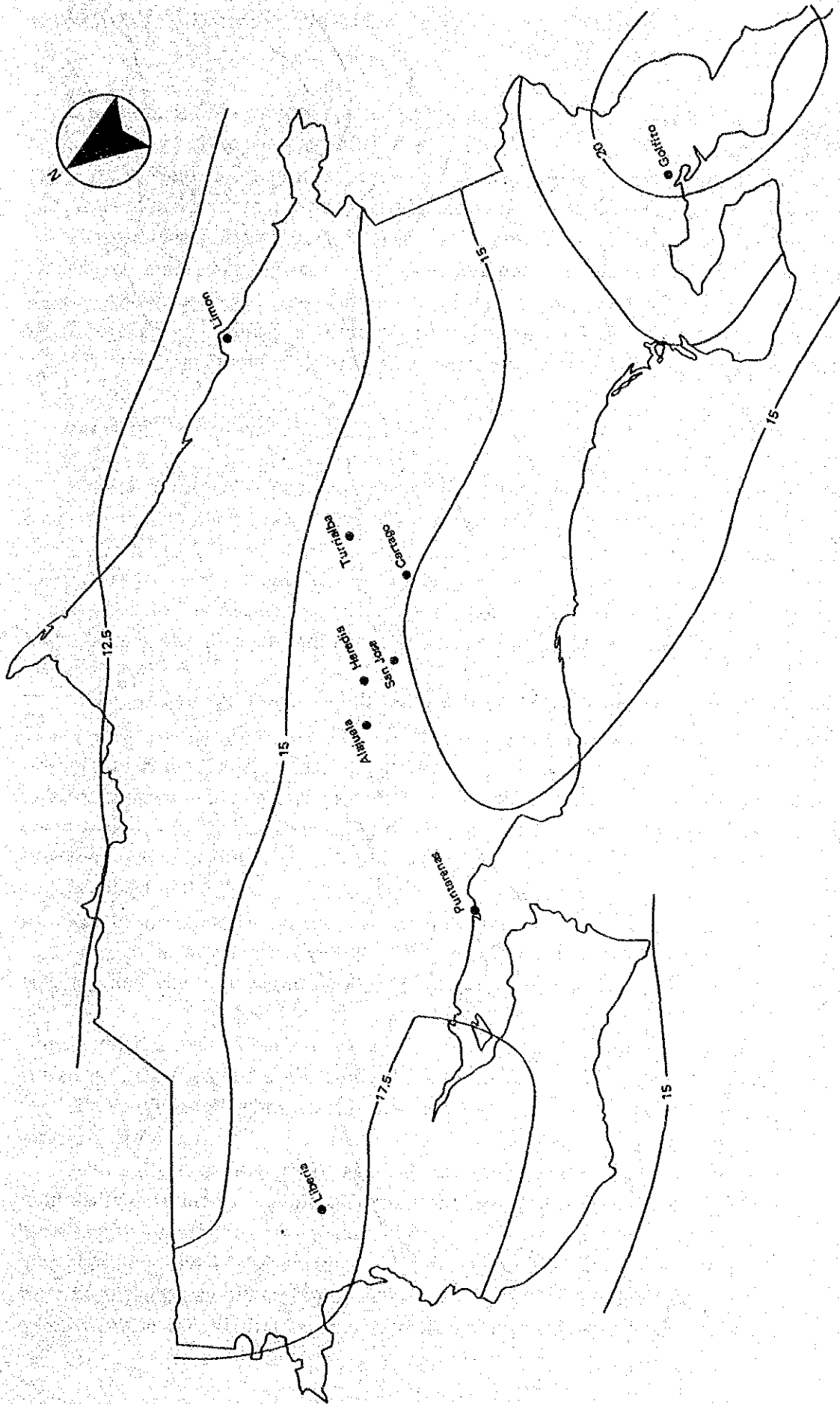
According to these figures, expected ground acceleration values are small along the Caribbean Coast and high in the Pacific Coast region, particularly near Golfito. The expected ground acceleration value in the Port of Caldera area is 0.15 G over a 50 year recurrence period, and $0.175 \sim 0.20$ G over a 100 year recurrence period, where G is equal to the acceleration of gravity.

5. 3 Tsunamis

It has been reported that the possiblity of tsunamis occuring in Costa Rica in slight considering the characteristics of the seismic faults which cause tsunamis.[8]

7) Christian P. Mortgat, Theodore C. Zsutty, Haresh C. Shah & Lester Lubetkin; A Study of Seismic Risk for Costa Rica, Rep. No. 25, The John A. Blume Earthquatke Engineering Center, Dep. of Civil Engineering, Stanford Univ., Apr. 1977, 359 p.
8) Luis Diego Morales M.; Los Temblores, sus Causas, Medición y Efectos, Setiembre Cientifico, Vol, 2, Sismos, Sep. 1985, pp. 43 ～ 83

Fig. IV-23 Iso-Acceleration Map (% of *G*) (Return Period 50 years)
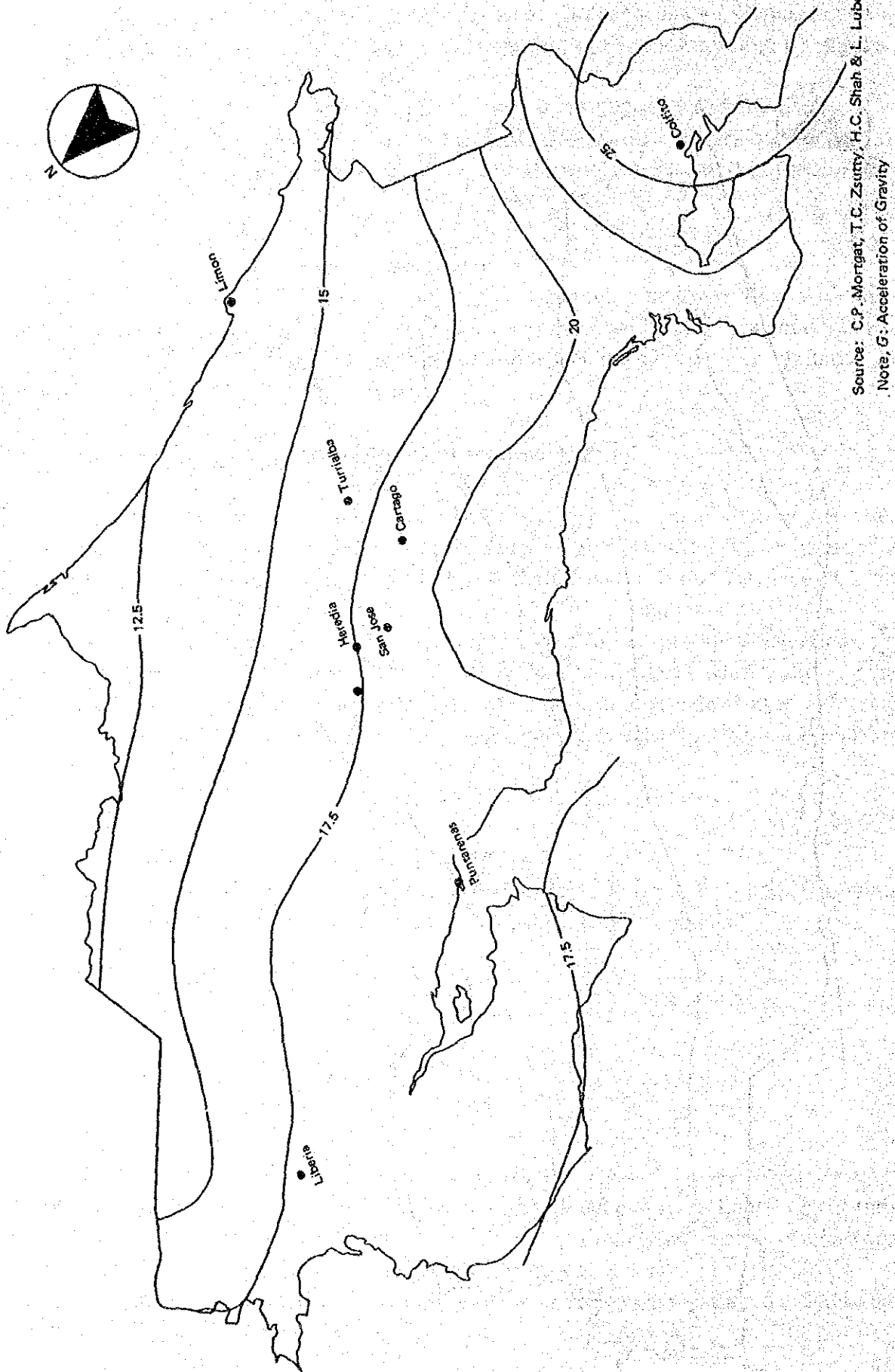
Source: C.P. Mortgat, T.C. Zsutty, H.C. Shah & L. Lubetkin

Note, *G*: Acceleration of Gravity

Fig. IV-24 Iso-Acceleration Map (% of G) (Return Period 100 Years)

Source: C.P.Morgat,T.C.Zsutty,H.C.Shah & L.Lubetkin
Note, G: Acceleration of Gravity